November 2, 2018

Table of Contents

List of Figures

Chapter 1

Radiation

1 Radiation

1.1 Basic Radiation Properties

Radiation: Energy transport by electromagnetic fields

Wave-particle duality and the radiative limit

Since we measure radiation only through the interaction with matter, wave propagation in vacuum is not all that interesting. When radiation interacts with matter, quantum mechanics can become important.

As Planck found, photon phase space is granular, with a fundamental quantized phase space volume of h^3. Photon energy is,

$$\boxed{E_\nu = h\,\nu} \tag{1.1}$$

Photons are relativistic, thus their momentum is directly proportional to their energy:

$$\boxed{P_\nu = \frac{h\nu}{c}} \tag{1.2}$$

Observables and basic definitions of radiation quantities

a) Specific intensity or surface brightness: I_ν

Define a quantity that describes completely how the measured energy dE depends

on $\vec{r}, \hat{\vec{k}}, \nu, t$ and describes the radiation field as completely as possible (neglecting polarization) given the information from the detector:

$$I_\nu(\vec{r}, t, \hat{\vec{k}}, \nu) \equiv \frac{dE}{d\nu\, dt\, d\Omega\, dA} \tag{1.3}$$

where the surface dA is taken **perpendicular** to the direction of the ray $\hat{k}$.

b) Mean intensity: J_ν

$\Rightarrow$ The zeroth moment of I_ν with respect to the polar angle $\cos\theta$:

$$J_\nu \equiv \frac{1}{4\pi} \int_{4\pi} d\Omega\, I_\nu \tag{1.4}$$

where the solid angle is,

$$d\Omega = \sin\theta d\theta d\phi \tag{1.5}$$

c) Specific flux: F_ν

$\Rightarrow$ The first moment of I_ν with respect to $\cos\theta$.

Energy flux at frequency ν across a surface dA, integrated over all photon directions (coming from both sides of the surface).

$$F_\nu \equiv \int_{4\pi} d\Omega\, \cos\theta\, I_\nu \tag{1.6}$$

where θ is measured relative to the normal of dA.

For an unresolved object, we can typically not determine the solid angle spanned by the object. The flux is therefore the most general quantity we can derive directly from any measurements for the object.

$$\boxed{F_\nu = 0 \;\text{ for isotropic radiation.}} \tag{1.7}$$

Sometimes it is useful to define a photon number flux. Since $e_\nu = h\nu$, this is simply

$$\Phi_\nu = F_\nu / h\nu \tag{1.8}$$

d) Total flux: F

$$F \equiv \int_0^\infty d\nu\, F_\nu = \left[\frac{dE}{dt\, dA}\right] \tag{1.9}$$

e) Radiation pressure: P_{rad} - Total momentum flux across dA

$$P_{rad} = \int_0^\infty d\nu \int_{4\pi} d\Omega \cos^2\theta \frac{I_\nu}{c} \tag{1.10}$$

f) Radiative energy density: u_ν - Amount of radiative energy contained per unit volume

$$u_\nu = \int du_\nu = \int_{4\pi} d\Omega \frac{I_\nu}{c} = \frac{dE}{dA\, ds\, d\nu} = \frac{dE}{dV\, d\nu} \tag{1.11}$$

where $ds = cdt$

The energy density of **blackbody radiation** per frequency interval is,

$$\boxed{u_\nu = \frac{8\pi\nu^2}{c^3} \frac{h\nu}{e^{h\nu/kT} - 1}} \tag{1.12}$$

The specific intensity, eq. (1.3), is related with the energy density via

$$I_\nu = c \frac{d\, u_\nu}{d\Omega} \tag{1.13}$$

Since the solid angle of a full sphere is 4π steradians, the intensity of blackbody radiation is therefore

$$\boxed{I_\nu = \frac{c}{4\pi} u_\nu = \frac{2h\,\nu^3}{c^2} \frac{1}{e^{h\nu/kT} - 1} \equiv B_\nu} \tag{1.14}$$

which is called as **Planck function**. In terms of wavelength, eq. (1.14) can be re-written by

$$B_\lambda = B_\nu \left|\frac{d\nu}{d\lambda}\right| = B_\nu \frac{c}{\lambda^2} = \frac{2h\, c^2}{\lambda^5} \frac{1}{e^{hc/\lambda kT} - 1} \tag{1.15}$$

For isotropic radiation, $u = 3\, P_{rad}$.

$$\begin{aligned} P_{rad} &= \int_{4\pi} d\Omega \cos^2\theta \frac{I}{c} = \frac{I}{c}\int_0^{\pi} \sin\theta\cos^2\theta d\theta \int_0^{2\pi} d\phi \\ &= \frac{2\pi I}{c}\int_{-1}^{1} x^2 dx = \frac{I}{c}\frac{4\pi}{3} \end{aligned} \tag{1.16}$$

where $x \equiv \cos\theta$

$$u = \int_{4\pi} d\Omega \frac{I}{c} = \frac{I}{c} 4\pi \tag{1.17}$$

Therefore,

$$\therefore u = 3\, P_{rad} \quad \text{for isotropic radiation} \tag{1.18}$$

g) Photon density: n_ν number of photons per unit frequency interval per unit volume.

$$n_\nu = \frac{u_\nu}{h\nu} \tag{1.19}$$

h) Luminosity: L_ν Specific (spectral) luminosity

$$L_\nu = \oint dA F_\nu = \left[\frac{dE}{dt\, d\nu}\right] \tag{1.20}$$

and total, "bolometric" luminosity:

$$L = \oint dA F = \left[\frac{dE}{dt}\right] \tag{1.21}$$

i) Spectral index:α

It is often convenient to plot spectra on a log-log plot in frequency, $\log F_\nu$ vs. $\log \nu$. Many emission process produce power-law type spectra over some frequency range,

$$F_\nu \propto \nu^{-\alpha} \tag{1.22}$$

which appear as straight lines in a log-log plot. It is then useful to define a local

spectral index

$$\alpha \equiv -\frac{\partial \log F_\nu}{\partial \log \nu} \tag{1.23}$$

sometimes it is also useful to define a photon index Γ

$$\Gamma \equiv -\frac{\partial \log \Phi_\nu}{\partial \log \nu} = -\frac{\partial \left(\log F_\nu - \log h\nu\right)}{\partial \log \nu} = \alpha + 1 \tag{1.24}$$

j) $\nu - \lambda$ conversions:

Given $\lambda\,\nu = c$, we can express specific quantity $f_\nu = df/d\nu$ with respect to wavelength instead:

$$f_\nu = \frac{df}{d\nu} = \frac{df}{d\lambda}\frac{d\lambda}{d\nu} \equiv f_\lambda \frac{\lambda^2}{c} \tag{1.25}$$

1.2 Basic laws

Stefan-Boltzmann law:

$$\boxed{u = a\,T^4} \tag{1.26}$$

which relates the total energy density of flux of a blackbody to its temperature.

Wien's law: The wavelength or frequency of the peak of a blackbody spectrum can be found by taking its derivative and equating to zero in eq. (1.26).

$$\begin{cases} \lambda_{max}\,T = 0.29 \text{ cm K} & (1.27) \\ h\,\nu_{max} = 2.8\,k\,T & (1.28) \end{cases}$$

Rayleigh-Jeans approximation: At frequencies ν much lower than the peak (i.e., at photon energies $h\nu \ll kT$) in blackbody spectrum eq. (1.26),

$$B_\nu \approx \frac{2\nu^2}{c^2}\,k\,T \quad \text{or,} \quad B_\lambda \approx 2\,c\,k\,T\lambda^{-4} \tag{1.29}$$

Wien tail: At frequencies ν much higher than the peak (i.e., at photon energies $h\nu \gg kT$)

in blackbody spectrum eq. (1.26),

$$B_\nu \sim e^{-h\nu/kT} \quad \text{or,} \quad B_\lambda \sim e^{-hc/\lambda kT} \tag{1.30}$$

Inverse square law:

$$F_\nu = \frac{L_\nu}{4\pi r^2} \tag{1.31}$$

Magnitudes:

Astronomers have long measured optical fluxes in logarithmic units (magnitudes). This was particularly convenient before the age of calculators but has stuck around somehow like many archaic scientific habits.

$$m_\lambda = -2.5 \log F_\lambda - C_\lambda \tag{1.32}$$
$$m_\nu = -2.5 \log F_\nu - C_\nu \tag{1.33}$$

where the constants $C_{\nu,\lambda}$ depend on the specific filter used and the assumed spectrum of the object.

1.3 Kinds of Radiation

hydrogen lines

The nth energy level of the hydrogen atom (n=1 is the ground state) is given by the Bohr formula,

$$E_n = -\frac{e^4 m_e}{2\hbar^2}\frac{1}{n^2} = -13.6\,\text{eV}\frac{1}{n^2} \tag{1.34}$$

The energy difference between two levels is

$$E_{n1,n2} = 13.6\,\text{eV}\left(\frac{1}{n_1^2} - \frac{1}{n_2^2}\right). \tag{1.35}$$

The wavelength of a photon emitted or absorbed in a radiative transition between two levels will be

$$\lambda_{n1,n2} = \frac{h\,c}{E_{n1,n2}} = \frac{911.5\text{Å}}{1/n_1^2 - 1/n_2^2}. \tag{1.36}$$

Table 1.1 Lyman series {transition to the ground level (n=1)}

label	transition	wavelength
Lyα	$2 \leftrightarrow 1$	1216 Å
Lyβ	$3 \leftrightarrow 1$	1025 Å
Lyγ	$4 \leftrightarrow 1$	972 Å

Up until the **Lyman continuum** (transition from infinity to the ground level ($n = \infty \leftrightarrow 1$), Ly_{con} = 911.5 Å.

Table 1.2 Balmer series {transition to the ground level (n=2)}

label	transition	wavelength
Hα	$3 \leftrightarrow 2$	6563 Å
Hβ	$4 \leftrightarrow 2$	4861 Å
Hγ	$5 \leftrightarrow 2$	4340 Å

Up until the **Balmer continuum** (transition from infinity to the second level ($n = \infty \leftrightarrow 2$), Ba_{con} = 3646 Å.

Thermal Bremstrahlung

to be described

Synchrotron

to be described

21 hydrogen line

to be described

Chapter 2

Fluid Dynamics

1 Fluid Dynamics

- $\partial/\partial t$: the rate of change of some physical quantity with respect to time at a fixed position in space.
- D/Dt (the material derivative): the rate of change of some quantity with respect to time but traveling along with the fluid.

  Let f be any quantity (e.g. density), then

$$\frac{Df}{Dt} = \frac{\partial f}{\partial t} + u \cdot \nabla f, \tag{2.1}$$

  where $u(r,t)$ is the velocity of the fluid at position r and time t.

1.1 Conservations

The continuity equation

Consider a volume V, which is fixed in space. The total mass of fluid in V is $\int_V \rho dV$. The time derivative of the mass in V is the mass flux into V across its surface S, i.e.

$$\frac{d}{dt}\int_V \rho dV = -\int_S (\rho \mathbf{u}) \cdot \mathbf{n}\, dS, \tag{2.2}$$

where $\mathbf{n}$ is the outward normal to the surface S. By using the divergence theorem, we obtain

$$\int_V \frac{\partial \rho}{\partial t} dV = -\int_S \rho \mathbf{u} \cdot \mathbf{n} dS = -\int_V \nabla \cdot (\rho \mathbf{u}) dV. \tag{2.3}$$

$$\therefore \frac{\partial \rho}{\partial t} + \nabla \cdot (\rho \mathbf{u}) = 0. \tag{2.4}$$

This is the continuity(or mass conservation) equation. Using eq 2.1 this can also be written as

$$\frac{D\rho}{Dt} + \rho \nabla \cdot \mathbf{u} = 0. \tag{2.5}$$

The momentum equation

By analogy, one can derive a momentum equation, or equation of motion, for the fluid by considering the rate of change of the total momentum of the fluid inside a volume V. The momentum of the fluid in V is $\int_V \rho \mathbf{u}\, dV$, and the rate of change of this momentum is equal to the net force acting on the fluid in volume V. These net force consists of two kinds; one is body force, such as gravity, which act on the particles inside V, and the other is surface force - forces exerted on the surface S of V by the surrounding fluid.

The former body force can be expressed as

$$\int_V \rho \mathbf{f}\, dV, \tag{2.6}$$

where **f** is the body force per unit mass (*i.e.* dimension: acceleration). The latter surface force is

$$-\int_S P\mathbf{n}\, dS, \tag{2.7}$$

where P is the pressure. Equating force to change of momentum we obtain

$$\frac{d}{dt}\int_V \rho \mathbf{u}\, dV = -\int_S P\mathbf{n}\, dS + \int_V \rho \mathbf{f}\, dV. \tag{2.8}$$

Since $\rho\, dV$, the mass of a fluid element, is invariant following the motion,

$$\frac{d}{dt}\int_V \rho \mathbf{u}\, dV = \int_V \rho \frac{D\mathbf{u}}{Dt}\, dV \tag{2.9}$$

and hence, applying the divergence theorem to the surface integral, we obtain

$$\int_V \rho \frac{D\mathbf{u}}{Dt}\, dV = \int_V \left(-\nabla P + \rho \mathbf{f}\right)\, dV. \tag{2.10}$$

$$\therefore\ \rho \frac{D\mathbf{u}}{Dt} = \rho \left(\frac{\partial \mathbf{u}}{\partial t} + (\mathbf{u} \cdot \nabla)\, \mathbf{u} \right) = -\nabla P + \rho \mathbf{f}. \tag{2.11}$$

This is the momentum equation for an inviscid fluid. Taking into account the viscous forces would add the right-hand side of the momentum equation with an additional term $\mu \left(\nabla^2 \mathbf{u} + \frac{1}{3} \nabla (\nabla \cdot \mathbf{u}) \right)$, where μ is dynamic viscosity.

The Energy equation

Taking a dot product of the equation of motion for a fluid, eq. 2.11, with the fluid velocity $\mathbf{u}$ yields

$$\frac{D}{Dt} \left(\frac{1}{2} \mathbf{u}^2 \right) = -\frac{1}{\rho} \mathbf{u} \cdot \nabla P + \mathbf{u} \cdot \mathbf{f}. \tag{2.12}$$

Eq. 2.12 says that the rate of change of the kinetic energy of a unit mass of fluid is equal to the rate at which work is done on the fluid by pressure and body forces. This is sometimes called the **mechanical energy equation**.

An equation for the total energy - kinetic and internal thermal energy - can be derived in the same manner as was the momentum equation. Let the internal energy per unit mass of fluid be U. Then the rate of change of kinetic plus internal energy of a material volume (*i.e.* one moving with the fluid) must be equal to the rate of work done on the fluid by surface and body forces, plus the rate at which heat is added to the fluid. Heat can be added in two ways: one is by its being generated at a rate ε per unit mass within the fluid volume (*e.g.* by nuclear reactions), while the second is by the flux of heat $\mathbf{F}$ into the volume from the surroundings (*e.g.* by radiation). Thus

$$\frac{d}{dt} \int_V \left(\frac{1}{2} \mathbf{u}^2 + U \right) \rho\, dV = \int_S \mathbf{u} \cdot (-P\mathbf{n})\, dS + \int_V \mathbf{u} \cdot \mathbf{f} \rho\, dV + \int_V \varepsilon \rho\, dV - \int_S \mathbf{F} \cdot \mathbf{n}\, dS. \tag{2.13}$$

In the same way as for the momentum equation, one rewrites all the surface integrals in this equation as volume integrals, using the divergence theorem. The resulting equation

holds for an arbitrary volume V and so one deduces that

$$\rho\left(\frac{D}{Dt}\left(\frac{1}{2}\mathbf{u}^2+\frac{DU}{Dt}\right)\right)=-\nabla\cdot(P\mathbf{u})+\rho\mathbf{u}\cdot\mathbf{f}+\rho\varepsilon-\nabla\cdot\mathbf{F}. \tag{2.14}$$

One can derive an equation for the thermal energy alone by dividing eq. 2.14 by the density and then subtracting the kinetic energy equation, eq. 2.12:

$$\frac{DU}{Dt}=\frac{P}{\rho^2}\frac{D\rho}{Dt}+\varepsilon-\frac{1}{\rho}\nabla\cdot\mathbf{F}. \tag{2.15}$$

Note that the divergence of $\nabla\cdot\mathbf{u}$ has been replaced by $-\rho^{-1}D\rho/Dt$ using the continuity equation, eq. 2.5.

1.2 Shock

Basic properties

ideal gas

The pressure is

$$P=n\,k\,T=\frac{\rho\,k\,T}{\mu\,m_H} \tag{2.16}$$

where μ is mean molecular weight.

Mean molecular weight The mean particle mass is

$$\bar{m}=\frac{n_1m_1+n_2m_2+n_3m_3+...}{n_1+n_2+n_3+...}=\frac{\rho}{n}=\mu\,m_H, \tag{2.17}$$

where μ is mean molecular weight.

The abundance of medium can be expressed as (X,Y,Z), which represent hydrogen, helium and heavy elements, respectively. By definition, the summation of them should be $\sum_i X_i = X+Y+Z=1$. The number density of hydrogen, helium, or an element of atomic mass number A will be

$$n_H=\frac{X\,\rho}{m_H},\quad n_{He}=\frac{Y\,\rho}{4\,m_H},\quad n_A=\frac{Z_A\,\rho}{A\,m_H} \tag{2.18}$$

In neutral limit, heavy elements is negligible. The number density of gas will be

$$n = n_H + n_{He} + n_A \simeq n_H + n_{He} = \frac{\rho}{m_H}\left(X + \frac{Y}{4}\right), \tag{2.19}$$

in other word, the mean molecular weight will be

$$\frac{1}{\mu} = X + \frac{Y}{4}. \tag{2.20}$$

In full-ionization limit, hydrgen produces 2 atoms (1 ion + 1 electron) and helium produces 3 atoms (1 ion + 2 electrons) and the heavy enough atoms produce the atomic number (ions+electrons) close to $A/2$.

$$n \simeq n_H + n_{He} + \sum \frac{A}{2} n_A = \frac{\rho}{m_H}\left(2X + \frac{3Y}{4} + \frac{1}{2}Z\right), \tag{2.21}$$

in other word, the mean molecular weight will be

$$\frac{1}{\mu} = 2X + \frac{3Y}{4} + \frac{1}{2}Z = \frac{1}{2}\left(3X + \frac{Y}{2} + 1\right). \tag{2.22}$$

For instance, if we apply the solar abundance (X=0.7, Y=0.28, Z=0.02) to the formula in two limits above, the mean molecular weight will be $\mu_{\text{solar,non}-\text{ionized}} = 1.3$ & $\mu_{\text{solar,ionized}} = 0.62$.

The general expression of mean molecular weight is

$$\frac{1}{\mu} = \frac{1}{\mu_I} + \frac{1}{\mu_e} = \sum \frac{X_i}{A_i} + \sum \frac{f_i Z_i X_i}{A_i}, \tag{2.23}$$

where μ_I, μ_e is the mean molecular weight of ion and electron, respectively, f_i is an ionization fraction.

Sound Speed C_s

In adiabatic situation $P = A\,\rho^\gamma$, where A is constant, the sound speed is

$$C_s^2 = \frac{\partial P}{\partial \rho} = \gamma \frac{P}{\rho}. \tag{2.24}$$

In isothermal situation ($\gamma = 1$),

$$C_s^2 = \frac{P}{\rho} = \frac{k\,T}{\mu\,m_H}. \tag{2.25}$$

Rankin-Hugoniot Condition

According to the conservation equations for mass, momentum and enery, the flow across the shock front has to satisfy the following jump conditions:

$$\begin{aligned} \rho_2\,u_2 &= \rho_1\,u_1 && (2.26)\\ \rho_2\,u_2^2 + P_2 &= \rho_1\,u_1^2 + P_1 && (2.27)\\ \frac{1}{2}u_2^2 + h_2 &= \frac{1}{2}u_1^2 + h_1 && (2.28) \end{aligned}$$

where the subscription 1 and 2 represent upstream and downstream, respectively, and h denotes the specific enthalpy which for a perfect gas satisfies the constituve relations:

$$h = \frac{\gamma}{\gamma-1}\frac{P}{\rho} = \frac{\gamma}{\gamma-1}\frac{k\,T}{\mu\,m_H}. \tag{2.29}$$

The upstream Mach number $\mathcal{M}_1 \equiv u_1/C_s$, where the sound speed of $C_s = \sqrt{\gamma\,P/\rho}$, the ratio of physical properties between downstream and upstream will be:

$$\begin{aligned} \frac{\rho_2}{\rho_1} &= \frac{u_1}{u_2} = \frac{(\gamma+1)\mathcal{M}_1^2}{(\gamma+1)+(\gamma-1)(\mathcal{M}_1^2-1)} && (2.30)\\ \frac{P_2}{P_1} &= \frac{(\gamma+1)+2\gamma(\mathcal{M}_1^2-1)}{\gamma+1} && (2.31)\\ \frac{T_2}{T_1} &= \frac{[(\gamma+1)+2\gamma(\mathcal{M}_1^2-1)][(\gamma+1)+(\gamma-1)(\mathcal{M}_1^2-1)]}{(\gamma+1)^2\mathcal{M}_1^2}. && (2.32) \end{aligned}$$

Note that $P_2 \geq P_1$, $\rho_2 \geq \rho_1$, and $T_2 \geq T_1$ if $\mathcal{M}_1 \geq 1$ (supersonic upstream). In the limit of a very strong shock ($\mathcal{M}_1 \to \infty$), the density jump is bounded by a finite value $(\gamma+1)/(\gamma-1)$, which is equals 4 if $\gamma = 5/3$. Simultaneously, the flow velocity slows down to $1/4$ of u_1. In this limit, the pressure and temperature jumps have no bound.

1.3 Instabilities

Thermal Instability

Gravitational Instability: Jean's Instability

See § 1.10.

Rayleigh-Taylor Instability

Kelvin-Helmholtz Instability

1.4 Turbulence

1.5 Magneto-hydrodynamics

Chapter 3

Thermo Dynamics

1 Thermo Dynamics

Noting that the volume per unit mass is just the reciprocal of the density, *i.e.* $V = æ^{-1}$, we recognise that the thermal energy equation (2.15) as a statement of **the first law of thermodynamics:**

$$dU = -PdV + \delta Q, \tag{3.1}$$

that is, the change in the internal energy is equal to the work-pdV done (on the fluid) plus the heat added. Note that p,V,U are properties of the fluid (in fact they are thermodynamic state variables) and we denote changes in them with the symbol d. In contrast, there is no such property as the heat content and so we cannot speak of the change of heat content. Instead, we can only speak of the heat added, and we therefore use a different notation, *i.e.* δQ. **The second law of thermodynamics** states that

$$\delta Q = TdS, \tag{3.2}$$

where S is a thermodynamic state variable, the *specific entropy* (*i.e.* the entropy per unit mass). Combining this with the first law, eq. 3.1, yields

$$dU = TdS - PdV. \tag{3.3}$$

1.1 Thermal Equilibrium

T.E.: Medium characterized by a single temperature and every process occurs at the same rate as its inverse process ($T_e = T_k = T_i = T_r$).

- T_e(excite T): Level population following by Boltzmann's distribution.

$$\frac{n_2}{n_1} = \frac{g_2}{g_1} e^{-E/kT_e} \tag{3.4}$$

- T_k(kinetic T): Particle velocity following by Boltzmann-Maxwellian velocity distribution.

$$f = 4\pi \left(\frac{m}{2\pi k T_k} \right)^{3/2} v^2 e^{-mv^2/2kT_k} \quad \text{or,} \quad \frac{1}{2} m v^2 = \frac{3}{2} k T_k \tag{3.5}$$

Doppler-Broadening: FWHM = $2\sqrt{2ln2}\,\sigma$, where $\sigma = \sqrt{kT/m}$

- T_i(ionization T): Ionizational fraction by Saha equation

$$\frac{n_{z+1} n_e}{n_z} = \frac{2 g_{z+1}}{g_z} \left(\frac{2\pi m_e k T_i}{h^2} \right)^{3/2} e^{-\chi/kT_i} \tag{3.6}$$

- T_r(radiational T): Radiation field by Planck function

$$B_\nu = \frac{2h\nu^3}{c^2} \frac{1}{e^{h\nu/kT_r} - 1} \tag{3.7}$$

L.T.E: ($T_e = T_k = T_i \neq T_r$)

cf) Brightness Temperature (T_b): Radio regime by Rayleigh-Jean's limit

$$B_\nu = \frac{2h\nu^3}{c^2} \frac{kT}{h\nu} \quad \text{or,} \quad T_b = B_\nu \frac{c^2}{2\nu^2 k}. \tag{3.8}$$

Chapter 4

Interstellar Medium

1 Cooling

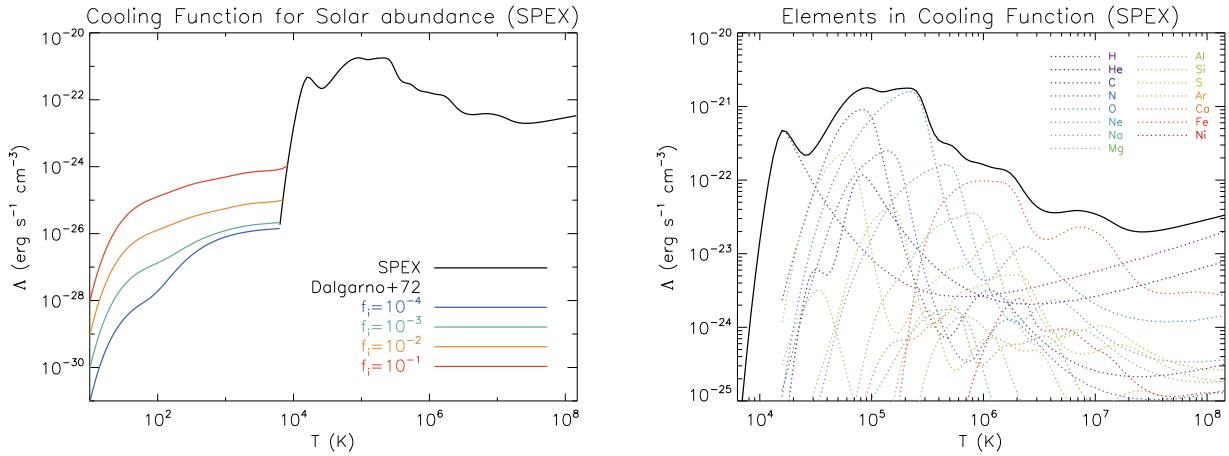

Figure 4.1 Cooling function in Collisional Ionization Equilibrium (CIE). I made use of SPEX pacakgeSchure et al. (2009). *left panel*: The cooling functions in low Temperature ($T < 10^4$ K) are computed from Dalgarno & McCray (1972), and the colored lines represent the cooling curves in different ionization fraction ($f_i = n_e/n_H$). *right panel*: The contribution of each elements on the cooling curve.

2 Heating

Chapter 5

Gravity

1 Gravity

1.1 Newtonian gravity

A mass m′ at position $\mathbf{r}'$ exerts on any other mass m at position $\mathbf{r}$ an attractive force $\mathbf{F} = m\mathbf{g}(\mathbf{r})$; the gravitational acceleration **g(r)** can be written as the gradient of a potential function, $\mathbf{g} = -\nabla\Psi$, where

$$\Psi = \frac{Gm'}{|\mathbf{r} - \mathbf{r}'|}, \tag{5.1}$$

$$\therefore |\nabla\Psi| = \frac{Gm'}{|\mathbf{r} - \mathbf{r}'|^2}. \tag{5.2}$$

Let S be a spherical surface of radius $\mathbf{r} - \mathbf{r}'$ centered at **r′**, then we have

$$\int_S \mathbf{n} \cdot \nabla\Psi dS = 4\pi G m'. \tag{5.3}$$

It can also be verified directly that the gravitational potential of our point mass (eq 5.32) satisfies $\nabla \cdot \nabla\Psi \equiv \nabla^2\Psi = 0$ (the Laplace equation) everywhere except for just one point, $\mathbf{r} = \mathbf{r}'$. By using divergence theorem, eq 5.33 can be expressed as,

$$\int_V \nabla^2\Psi \, dV = 4\pi G \int_V \rho \, dV, \tag{5.4}$$

where V is volume inside S. Since V is arbitrary, this equation can be rewritten as a partial differential equation, **Poisson's equation:**

$$\nabla^2\Psi = 4\pi G\rho \tag{5.5}$$

1.2 Simple models of astrophysical fluid and their motions

In the previous lecture we established the continuity equation (2.5), the momentum equation (2.11), the energy equation (2.14), and Poisson's equation (5.35). Assuming that the only body forces are due to self-gravity, so that $\mathbf{f} = -\nabla\Psi$ in eq. 2.11, these equations are:

$$\left[\begin{array}{rl} \dfrac{D\rho}{Dt} + \rho\nabla\cdot\mathbf{u} = 0, & (5.6)\\ \rho\dfrac{D\mathbf{u}}{Dt} = -\nabla P - \rho\nabla\Psi, & (5.7)\\ \dfrac{DU}{Dt} - \dfrac{P}{\rho^2}\dfrac{D\rho}{Dt} = \varepsilon - \dfrac{1}{\rho}\nabla\cdot\mathbf{F}, & (5.8)\\ \nabla^2\Psi = 4\pi G\rho. & (5.9) \end{array}\right]$$

Note that these contain seven dependent variables (ρ, P, Ψ, U,and three components of $\mathbf{u}$). The three equations from momentum equation, together with the rest equations, provide six equations, and a seventh is the equation of state (*e.g.* that for an ideal gas) which provides a relation between any three thermodynamic state variables, so that for instance the internal energy U and temperature T can be written in terms of P and ρ.(ε and $\mathbf{F}$ are assumed to be known functions of the other variables). Thus one might hope in principle to solve these equations, given suitable boundary conditions. In practice this set of equations is intractable to exact solution, and one must resort to numerical solutions. Even these can be extremely problematic so that, for example, understanding turbulent flows is still a very challenging research area. Moreover, an analytic solution to a somewhat idealized problem may teach one much more than a numerical solution. One useful idealization is where we assume that the fluid velocity and all time derivatives are zero. These are called equilibrium solutions and describe a steady an astrophysical system evolves may be very long, so that at any particular time the state of many astrophysical fluid bodies may be well represented by an equilibrium model. Even when the dynamical behaviour of the body is important, it can often be described in terms of small departures from an equilibrium state.

1.3 Hydrostatic equilibrium for a self-gravitating body

If we suppose that $\mathbf{u} = 0$ every where, and that all quantities are independent of time, eq. 5.38 becomes

$$\nabla P + \rho \nabla \Psi = 0 \tag{5.10}$$

the continuity equation becomes trivial. A fluid satisfying eq. 5.41 is said to be in **hydrostatic equilibrium**. If it is self-gravitating (so that Ψ is determined by the density distribution within the fluid), then eq. 5.40 must also be satisfied.

Putting $\mathbf{u} = 0$ and $\partial/\partial t$=0, *i.e.* $D/Dt = 0$, in eq. 5.39, we obtain that the heat sources given by ε must be exactly balance by the heat flux term $\rho^{-1}\nabla \cdot \mathbf{F}$. If this holds, then the fluid is also said to be in thermal equilibrium (See §1.1).

1.4 The formation of protostars

Stellar time scales

a) dynamical time scale

The length of time over which changes in one part of a body can be communicated to the rest of that body. That is also called, freefall time scale.

Assuming $|dP/dr| \ll GM_r\rho/r^2$, where M_r is the mass of the spherical cloud,

$$\frac{d^2r}{dt^2} = -G\frac{M_r}{r^2} = -\frac{G}{r^2}\frac{4\pi}{3}\rho_0 r_0^3, \tag{5.11}$$

where, r_0 and ρ_0 is the initial radius and density of the sphere. Multiplying the velocity of the surface of the sphere for both sides,

$$\frac{dr}{dt}\frac{d^2r}{dt^2} = -\frac{G}{r^2}\frac{4\pi}{3}\rho_0 r_0^3\frac{dr}{dt}, \tag{5.12}$$

which can be integrated to give

$$\frac{1}{2}\left(\frac{dr}{dt}\right)^2 = \left(\frac{4\pi}{3}G\rho_0 r_0^3\right)\frac{1}{r} + C_1. \tag{5.13}$$

where C_1 can be evaluated by, $dr/dt = 0$ when $r = r_0$. This gives

$$C_1 = -\frac{4\pi}{3}G\rho_0 r_0^2. \tag{5.14}$$

therefore,

$$\frac{dr}{dt} = -\left[\frac{8\pi}{3} G\rho_0 r_0^2 \left(\frac{r_0}{r} - 1\right)\right]^{1/2}. \tag{5.15}$$

Substituting $\theta \equiv r/r_0$ and $K \equiv \left(\frac{8\pi}{3} G\rho_0\right)^{1/2}$ gives,

$$\frac{d\theta}{dt} = -K\left(\frac{1}{\theta} - 1\right)^{1/2}. \tag{5.16}$$

Making another substitution, $\theta \equiv \cos^2\phi$, then

$$\cos^2\phi \frac{d\phi}{dt} = \frac{K}{2}. \tag{5.17}$$

This will be integrated to yield

$$\frac{\sin 2\phi}{4} + \frac{\phi}{2} = \frac{K}{2}t + C_2. \tag{5.18}$$

where C_2 can be evaluated by, $r = r_0$ when $t = 0$ implying $\theta = 1$ or $\phi = 0$ at the beginning of the collapse, then gives $C_2 = 0$.

Consequently, the freefall time scale or dynamical time scale can be calculated by, $\theta = 0$ or $\phi = \pi/2$,

$$\begin{aligned} t_{dyn} = t_{ff} &= \frac{\pi}{2K} \\ &= \left(\frac{3\pi}{32}\frac{1}{G\rho_0}\right)^{1/2}. \end{aligned} \tag{5.19}$$

b) thermal time scale

The time scale on which the star would contract if its nuclear energy sources were turned off. And it is also called, kelvin-Helmholtz time scale:

$$t_{KH} \approx \frac{GM^2/R_*}{L}. \tag{5.20}$$

c) nuclear time scale The heat released by fusing a mass $\triangle Mc^2$. Therefore the time

required to exhaust all the star's hydrogen is

$$t_{nuc} = \frac{0.007Mc^2}{L} \tag{5.21}$$

Jean's Instability

Two methods will be described to derive Jean's Mass.

a) From virial theorem

The potential energy is,

$$dU = G\frac{M_{interior}M_{shell}}{r}. \tag{5.22}$$

Integrating the equation,

$$U = G\int_R^0 \frac{4/3\pi r^3\rho\ 4\pi r^2\rho\, dr}{r} = -\frac{3}{5}\frac{GM^2}{R}, \tag{5.23}$$

where $\rho = M/(\frac{4}{3}\pi R^3)$.

The kinetic energy is

$$K = N_H\ \frac{3}{2}kT = \frac{M}{\mu m_H}\ \frac{3}{2}kT. \tag{5.24}$$

Using a virial theorem, 2K+U=0,

$$\frac{3}{5}\frac{GM^2}{R} = 3\frac{MkT}{\mu m_H}, \tag{5.25}$$

therefore, the Jean's mass can be calculated to

$$M_J = \left(\frac{5kT}{G\mu m_H}\right)^{3/2}\left(\frac{3}{4\pi\rho}\right)^{1/2}, \tag{5.26}$$

because $R = \left(M/(\frac{4}{3}\pi\rho)\right)^{1/3}$. The following length is

$$R_J = \left(\frac{M_J}{\frac{4}{3}\pi\rho}\right)^{1/3} = \left(\frac{5kT}{G\mu m_H}\right)^{1/2}\left(\frac{3}{4\pi\rho}\right)^{1/2}, \tag{5.27}$$

where the Jean's length, $\lambda_J = 2R_J$.

b) From freefall time

The freefall time scale is, from Eqn. 5.50,

$$t_{ff} = \left(\frac{3\pi}{32}\frac{1}{G\rho_0}\right)^{1/2}. \tag{5.28}$$

In order to collapse the cloud, the freefall time scale should be less than the crossing time scale which is the time scale in which the information propagates from edge to edge, that is

$$t_{cs} = \frac{\lambda_J}{Cs}, \tag{5.29}$$

where Cs is the sound speed of $\sqrt{\frac{kT}{\mu m_H}}$. As a result,

$$\left(\frac{3\pi}{32}\frac{1}{G\rho_0}\right)^{1/2} = \frac{\lambda_J}{Cs} \tag{5.30}$$

or,

$$\lambda_J = \left(\frac{3\pi kT}{32G\rho\mu m_H}\right)^{1/2}. \tag{5.31}$$

1.5 Special relativity

to be described

1.6 General relativity

to be described sectionGravity

1.7 Newtonian gravity

A mass m' at position $\mathbf{r}'$ exerts on any other mass m at position $\mathbf{r}$ an attractive force $\mathbf{F} = m\mathbf{g}(\mathbf{r})$; the gravitational acceleration $\mathbf{g}(\mathbf{r})$ can be written as the gradient of a potential

function, $\mathbf{g} = -\nabla\Psi$, where

$$\Psi = \frac{Gm'}{|\mathbf{r} - \mathbf{r}'|}, \tag{5.32}$$

$$\therefore |\nabla\Psi| = \frac{Gm'}{|\mathbf{r} - \mathbf{r}'|^2}. \tag{5.33}$$

Let S be a spherical surface of radius $|\mathbf{r} - \mathbf{r}'|$ centered at $\mathbf{r}'$, then we have

$$\int_S \mathbf{n} \cdot \nabla\Psi dS = 4\pi G m'. \tag{5.34}$$

It can also be verified directly that the gravitational potential of our point mass (eq 5.32) satisfies $\nabla \cdot \nabla\Psi \equiv \nabla^2\Psi = 0$ (the Laplace equation) everywhere except for just one point, $\mathbf{r} = \mathbf{r}'$. By using divergence theorem, eq 5.33 can be expressed as,

$$\int_V \nabla^2\Psi \, dV = 4\pi G \int_V \rho \, dV, \tag{5.35}$$

where V is volume inside S. Since V is arbitrary, this equation can be rewritten as a partial differential equation, **Poisson's equation:**

$$\nabla^2\Psi = 4\pi G\rho \tag{5.36}$$

1.8 Simple models of astrophysical fluid and their motions

In the previous lecture we established the continuity equation (2.5), the momentum equation (2.11), the energy equation (2.14), and Poisson's equation (5.35). Assuming that the only body forces are due to self-gravity, so that $\mathbf{f} = -\nabla\Psi$ in eq. 2.11, these equations are:

$$\left[\begin{array}{rl}
\dfrac{D\rho}{Dt} + \rho\nabla \cdot \mathbf{u} = 0, & (5.37)\\
\rho\dfrac{D\mathbf{u}}{Dt} = -\nabla P - \rho\nabla\Psi, & (5.38)\\
\dfrac{DU}{Dt} - \dfrac{P}{\rho^2}\dfrac{D\rho}{Dt} = \varepsilon - \dfrac{1}{\rho}\nabla \cdot \mathbf{F}, & (5.39)\\
\nabla^2\Psi = 4\pi G\rho. & (5.40)
\end{array}\right]$$

Note that these contain seven dependent variables (ρ, P, Ψ, U,and three components of $\mathbf{u}$). The three equations from momentum equation, together with the rest equations, provide six equations, and a seventh is the equation of state (*e.g.* that for an ideal gas) which provides a relation between any three thermodynamic state variables, so that for instance the internal energy U and temperature T can be written in terms of P and ρ.(ε and $\mathbf{F}$ are assumed to be known functions of the other variables). Thus one might hope in principle to solve these equations, given suitable boundary conditions. In practice this set of equations is intractable to exact solution, and one must resort to numerical solutions. Even these can be extremely problematic so that, for example, understanding turbulent flows is still a very challenging research area. Moreover, an analytic solution to a somewhat idealized problem may teach one much more than a numerical solution. One useful idealization is where we assume that the fluid velocity and all time derivatives are zero. These are called equilibrium solutions and describe a steady an astrophysical system evolves may be very long, so that at any particular time the state of many astrophysical fluid bodies may be well represented by an equilibrium model. Even when the dynamical behaviour of the body is important, it can often be described in terms of small departures from an equilibrium state.

1.9 Hydrostatic equilibrium for a self-gravitating body

If we suppose that $\mathbf{u} = 0$ every where, and that all quantities are independent of time, eq. 5.38 becomes

$$\nabla P + \rho \nabla \Psi = 0 \tag{5.41}$$

the continuity equation becomes trivial. A fluid satisfying eq. 5.41 is said to be in **hydrostatic equilibrium**. If it is self-gravitating (so that Ψ is determined by the density distribution within the fluid), then eq. 5.40 must also be satisfied.

Putting $\mathbf{u} = 0$ and $\partial/\partial t$=0, *i.e.* D/Dt=0, in eq. 5.39, we obtain that the heat sources given by ε must be exactly balance by the heat flux term $\rho^{-1}\nabla \cdot \mathbf{F}$. If this holds, then the fluid is also said to be in thermal equilibrium (See §1.1).

1.10 The formation of protostars

Stellar time scales

a) dynamical time scale

The length of time over which changes in one part of a body can be communicated to the rest of that body. That is also called, freefall time scale.

Assuming $|dP/dr| \ll GM_r\rho/r^2$, where M_r is the mass of the spherical cloud,

$$\frac{d^2r}{dt^2} = -G\frac{M_r}{r^2} = -\frac{G}{r^2}\frac{4\pi}{3}\rho_0 r_0^3, \tag{5.42}$$

where, r_0 and ρ_0 is the initial radius and density of the sphere. Multiplying the velocity of the surface of the sphere for both sides,

$$\frac{dr}{dt}\frac{d^2r}{dt^2} = -\frac{G}{r^2}\frac{4\pi}{3}\rho_0 r_0^3\frac{dr}{dt}, \tag{5.43}$$

which can be integrated to give

$$\frac{1}{2}\left(\frac{dr}{dt}\right)^2 = \left(\frac{4\pi}{3}G\rho_0 r_0^3\right)\frac{1}{r} + C_1. \tag{5.44}$$

where C_1 can be evaluated by, $dr/dt = 0$ when $r = r_0$. This gives

$$C_1 = -\frac{4\pi}{3}G\rho_0 r_0^2. \tag{5.45}$$

therefore,

$$\frac{dr}{dt} = -\left[\frac{8\pi}{3}G\rho_0 r_0^2\left(\frac{r_0}{r} - 1\right)\right]^{1/2}. \tag{5.46}$$

Substituting $\theta \equiv r/r_0$ and $K \equiv \left(\frac{8\pi}{3}G\rho_0\right)^{1/2}$ gives,

$$\frac{d\theta}{dt} = -K\left(\frac{1}{\theta} - 1\right)^{1/2}. \tag{5.47}$$

Making another substitution, $\theta \equiv \cos^2\phi$, then

$$\cos^2\phi\frac{d\phi}{dt} = \frac{K}{2}. \tag{5.48}$$

This will be integrated to yield

$$\frac{\sin 2\phi}{4} + \frac{\phi}{2} = \frac{K}{2}t + C_2. \tag{5.49}$$

where C_2 can be evaluated by, $r = r_0$ when $t = 0$ implying $\theta = 1$ or $\phi = 0$ at the beginning of the collapse, then gives $C_2 = 0$.

Consequently, the freefall time scale or dynamical time scale can be calculated by, $\theta = 0$ or $\phi = \pi/2$,

$$\begin{aligned} t_{dyn} = t_{ff} &= \frac{\pi}{2K} \\ &= \left(\frac{3\pi}{32}\frac{1}{G\rho_0}\right)^{1/2}. \end{aligned} \tag{5.50}$$

b) thermal time scale

The time scale on which the star would contract if its nuclear energy sources were turned off. And it is also called, kelvin-Helmholtz time scale:

$$t_{KH} \approx \frac{GM^2/R_*}{L}. \tag{5.51}$$

c) nuclear time scale The heat released by fusing a mass $\triangle Mc^2$. Therefore the time required to exhaust all the star's hydrogen is

$$t_{nuc} = \frac{0.007Mc^2}{L} \tag{5.52}$$

Jean's Instability

Two methods will be described to derive Jean's Mass.

a) From virial theorem

The potential energy is,

$$dU = G\frac{M_{interior}M_{shell}}{r}. \tag{5.53}$$

Integrating the equation,

$$U = G\int_R^0 \frac{4/3\pi r^3\rho\ 4\pi r^2\rho\, dr}{r} = -\frac{3}{5}\frac{GM^2}{R}, \tag{5.54}$$

where $\rho = M/(\frac{4}{3}\pi R^3)$.

The kinetic energy is

$$K = N_H\ \frac{3}{2}kT = \frac{M}{\mu m_H}\ \frac{3}{2}kT. \tag{5.55}$$

Using a virial theorem, 2K+U=0,

$$\frac{3}{5}\frac{GM^2}{R} = 3\frac{MkT}{\mu m_H}, \tag{5.56}$$

therefore, the Jean's mass can be calculated to

$$M_J = \left(\frac{5kT}{G\mu m_H}\right)^{3/2}\left(\frac{3}{4\pi\rho}\right)^{1/2}, \tag{5.57}$$

because $R = \left(M/(\frac{4}{3}\pi\rho)\right)^{1/3}$. The following length is

$$R_J = \left(\frac{M_J}{\frac{4}{3}\pi\rho}\right)^{1/3} = \left(\frac{5kT}{G\mu m_H}\right)^{1/2}\left(\frac{3}{4\pi\rho}\right)^{1/2}, \tag{5.58}$$

where the Jean's length, $\lambda_J = 2R_J$.

b) From freefall time

The freefall time scale is, from Eqn. 5.50,

$$t_{ff} = \left(\frac{3\pi}{32}\frac{1}{G\rho_0}\right)^{1/2}. \tag{5.59}$$

In order to collapse the cloud, the freefall time scale should be less than the crossing time scale which is the time scale in which the information propagates from edge to edge, that is

$$t_{cs} = \frac{\lambda_J}{Cs}, \tag{5.60}$$

where Cs is the sound speed of $\sqrt{\frac{kT}{\mu m_H}}$. As a result,

$$\left(\frac{3\pi}{32}\frac{1}{G\rho_0}\right)^{1/2} = \frac{\lambda_J}{Cs} \tag{5.61}$$

or,

$$\lambda_J = \left(\frac{3\pi kT}{32G\rho\mu m_H}\right)^{1/2}. \tag{5.62}$$

1.11 Special relativity

to be described

1.12 General relativity

to be described

Chapter 6

Galactic Dynamics

1 Galactic Dynamics

1.1 Stellar distribution

The surface brightness (stellar components) of elliptical galaxy falls off smoothly with radius, and it can be fitted by some empirical profiles:

1) Sérsic profile

$$I(r) = I_e \exp\left\{-\nu_n \left[\left(\frac{r}{r_e}\right)^{1/n} - 1\right]\right\}, \tag{6.1}$$

where, r_e is effective radius, the radius of the isophote containing half of the total luminosity.

2) De Vaucouleurs profile

When $n = 4$, $\nu_4 = 7.66925$, the Sérsic profile [eq. (6.1)] becomes de Vaucouleurs profile,

$$I(r) = I_e \exp\left\{-\nu_4 \left[\left(\frac{r}{r_e}\right)^{1/4} - 1\right]\right\}. \tag{6.2}$$

3) King profile

King profile was developed from the singular isothermal sphere model, at which the distribution function follows the balance between the gravitational potential and velocity dispersion (analogue to the hydrostatic equilibrium sphere with adiabatic index of $\gamma =$

1).

$$I(r) = K \left\{ \left[1 + \left(\frac{r}{r_c} \right)^2 \right]^{-1/2} - \left[1 + \left(\frac{r_t}{r} \right)^2 \right]^{-1/2} \right\}^2, \tag{6.3}$$

where r_c is the core radius $\left[\frac{I(r=0)}{I(r=r_c)} = 2 \right]$, r_t is the tidal radius where is considered as outermost limit of the system by observers, and K is the scale factor.

This profile gives a very good representation of star counts in tidally-limited globular clusters and low-density spheroidal galaxies.

4) Exponential profile

Disks of spiral galaxies are known to show profiles described well by the exponential law:

$$I(r) = I_0 \exp\left(-\frac{r}{h} \right), \tag{6.4}$$

where h is the exponential scale length.

1.2 Dark matter profile: Two-power density models binney & tremaine (1987)

Numerical simulations of the clustering of dsrk matter particles suggest that the mass density with dark halo has a similar structure. Mostly, the two-power density models has been applied:

$$\rho(r) = \frac{\rho_0}{(r/a)^\alpha (1 + r/a)^{\beta - \alpha}}. \tag{6.5}$$

According to the sets of (α, β), the model can be classified with Jaffe, Hernquist, and NFW profiles. The mass interior to radidus r is

$$M(r) = 4\pi\rho_0 a^3 \int_0^{r/a} ds \, \frac{s^{2-\alpha}}{(1+s)^{\beta-\alpha}}. \tag{6.6}$$

1) Jaffe profile

$\alpha = 2$ and $\beta = 4$ in eq. (6.5). Therefore, from eq. (6.6), the mass profile becomes

$$M(r) = 4\pi\rho_0 a^3 \frac{r/a}{1 + r/a}, \tag{6.7}$$

and the potential becomes

$$\begin{aligned}\Phi(r) &= -G\int_r^\infty dr\,\frac{M(r)}{r^2} \\ &= -4\pi\rho_0\,a^2\,\ln(1+a/r).\end{aligned} \tag{6.8}$$

2) Hernquist profile

$\alpha = 1$ and $\beta = 4$ in eq. (6.5). Therefore, from eq. (6.6), the mass profile becomes

$$M(r) = 4\pi\rho_0\,a^3\frac{(r/a)^2}{2(1+r/a)^2}, \tag{6.9}$$

and the potential becomes

$$\begin{aligned}\Phi(r) &= -G\int_r^\infty dr\,\frac{M(r)}{r^2} \\ &= -4\pi\rho_0\,a^2\,\frac{1}{2(1+r/a)}.\end{aligned} \tag{6.10}$$

3) NFW profile

NFW profile is named from Navarro, Frenk, & White (1995). $\alpha = 1$ and $\beta = 3$ in eq. (6.5). Therefore, from eq. (6.6), the mass profile becomes

$$M(r) = 4\pi\rho_0\,a^3\left[\ln(1+r/a) - \frac{r/a}{1+r/a}\right], \tag{6.11}$$

and the potential becomes

$$\begin{aligned}\Phi(r) &= -G\int_r^\infty dr\,\frac{M(r)}{r^2} \\ &= -4\pi\rho_0\,a^2\,\frac{\ln(1+r/a)}{r/a}.\end{aligned} \tag{6.12}$$

1.3 Fundamental Plane

Fundamental plane is an empirical relationship of observed elliptical galaxies between the effective radius r_e (see §1.1), average surface brightness I (or Luminosity L_B), and

central velocity dispersion σ_0 (Fig. 6.1).

$$\log r_e = A \log \sigma_0 + B \log L_B + C. \tag{6.13}$$

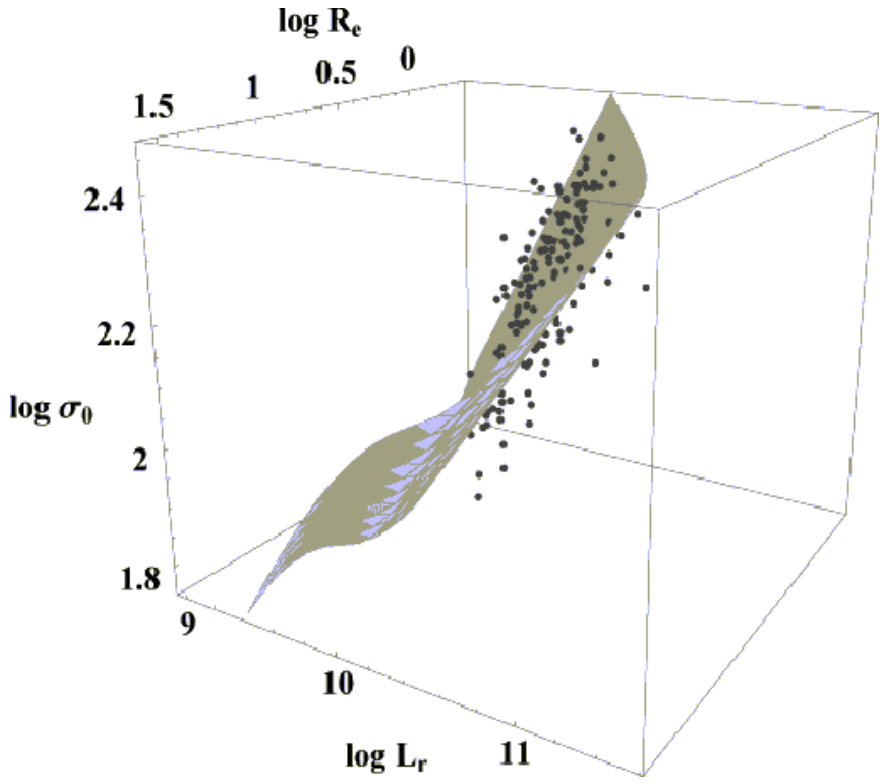

Figure 6.1 3 dimensional space (r_e, σ_0, L) of Fundamental Plane

1.4 Faber-Jackson relation

This relation is an empirical power-law relation between the luminosity L and the central stellar velocity dispersion σ_0 of elliptical galaxies.

The theoretical derivation requires some assumptions:

The gravitational potential for uniform sphere (constant density; see §1.2) is

$$U = -\frac{3}{5}\frac{G M}{R}. \tag{6.14}$$

And the kinetic energy is

$$K = \frac{3}{2} M \sigma_0^2, \tag{6.15}$$

where σ_0 is 1-dimensional velocity dispersion ($3\sigma_0^2 = V^2$ where V is total velocity dispersion). From the virial therom ($2K + U = 0$), it follows

$$\sigma^2 = \frac{1}{5}\frac{G\,M}{R}. \tag{6.16}$$

Assuming the constant mass to light ratio $\Upsilon = M/L$, then

$$R = \frac{1}{5}\frac{\Upsilon L\,G}{R}. \tag{6.17}$$

If we assume that the surface brightness $I = L/(4\pi R^2)$ is constant (highly unlikely), then

$$L = \frac{25\,\sigma^4}{4\pi\,G^2\,I\,\Upsilon^2} \propto \sigma^4. \tag{6.18}$$

Since the assumptions during the derivation are poor, the empirical power varies between 3 (less massive galaxies) and 15 (more massive galaxies).

1.5 Tully-Fisher relation

The rotation rate of spiral galaxies in the flat part of the circular-speed curve is related to their luminosity.

1.6 Nearly circular orbits: Epicycle frequency

In disk galaxies, many stars are on nearly circular orbits. We define

$$x \equiv r - r_g, \tag{6.19}$$

where r_g is the guiding center radius for an orbit. The effective potential is

$$\Phi_{\text{eff}} = \Phi + \frac{l^2}{2\,r^2}, \tag{6.20}$$

where l is a specific angular momentum $l = r\,v_\phi$, and v_ϕ is rotation velocity. Expanding Φ_{eff} in a Taylor series results in

$$\Phi_{\text{eff}}(r) = \Phi_{\text{eff}}(r_g) + \left.\frac{\partial\Phi_{\text{eff}}}{\partial r}\right|_{r=r_g} x + \frac{1}{2}\left.\frac{\partial^2\Phi_{\text{eff}}}{\partial r^2}\right|_{r=r_g} x^2 + O(x^2). \tag{6.21}$$

The first order term (second term in RHS) vanishes because $\Phi_{\rm eff}$ is assumed to be symmetic about $r = r_g$. So the eq. (6.21) can be approximated to

$$\Phi_{\rm eff}(r) \simeq \Phi_{\rm eff}(r_g) + \frac{1}{2}\left.\frac{\partial^2 \Phi_{\rm eff}}{\partial r^2}\right|_{r=r_g} x^2 \tag{6.22}$$

The equation of motion is

$$\ddot{x} = -\frac{\Phi_{\rm eff}}{x} = -\left.\frac{\partial^2 \Phi_{\rm eff}}{\partial r^2}\right|_{r=r_g} x \tag{6.23}$$

$$= -\kappa^2\, x, \tag{6.24}$$

where κ is called *epicycle frequency*.

$$\kappa^2(r_g) = \left.\frac{\partial^2 \Phi_{\rm eff}}{\partial r^2}\right|_{r=r_g} = \left.\frac{\partial^2 \Phi}{\partial r^2}\right|_{r=r_g} + \frac{3\,l^2}{r_g^4}. \tag{6.25}$$

Since the circular frequency is related with the gravitational force,

$$\frac{\partial \Phi}{\partial r} = r\,\Omega^2, \tag{6.26}$$

where $\Omega = l/r^2$ is an angular frequency of the circular orbit. Plugging into eq. (6.25) gives

$$\kappa^2(r_g) = \left(r\frac{d\,\Omega^2}{d\,r} + 4\,\Omega^2\right)_{r=r_g} \tag{6.27}$$

$$= \left[\frac{1}{r^3}\frac{d}{d\,r}\left(r^4\,\Omega^2\right)\right]_{r=r_g}. \tag{6.28}$$

If we assumes that the angular frequency has a power-law relationship with the radius ($\Omega \sim r^q$), the eq. (6.27) can be expressed as

$$\kappa^2 = (4+2q)\,r^{2q} = (4+2q)\,\Omega^2. \tag{6.29}$$

Note the several examples of the epicycle frequency:

$$\begin{cases} \text{Rigid rotation} : \Omega \sim R^0 \rightarrow \kappa^2 = 4\Omega^2 & (6.30) \\ \text{Keplerian rotation} : \Omega \sim R^{-3/2} \rightarrow \kappa^2 = \Omega^2 & (6.31) \\ \text{Flat rotation} : \Omega \sim R^{-1} \rightarrow \kappa^2 = 2\Omega^2 & (6.32) \end{cases}$$

In the rigid and Keplerian rotations, the epicycle motion is closed, but in the flat rotation it is not closed.

1.7 Luminosity function: Schechter law

The luminosity function $\phi(L)$ describes the relative numbers of galaxies of different luminosities, and is defined so that $\phi(L)\,dL$ is the number of galaxies in the luminosity interal $L \rightarrow L + dL$ in a representative unit volume of the universe. The analytic approximation is know as Schechter law:

$$\phi(L)\,dL = \phi_\star \left(\frac{L}{L_\star}\right)^\alpha \exp\left(-\frac{L}{L_\star}\right)\frac{dL}{L}, \tag{6.33}$$

where $\phi_\star \simeq 4.9 \times 10^{-3}\,\mathrm{Mpc}^{-3}$, $\alpha = -1.1$, and $L_\star \simeq 2.9 \times 10^{10}\,L_\odot$ in the R band.

1.8 Star Formation Rate: Kennicutt-Schmidt Law

Kennicutt-Schmidt law is the empirical relationship between the global star formation in a galaxy and $\Sigma_{\mathrm{gas,disk}}$ the gas surface density averaged over the "optical disk" of the galaxy, finding that the star formation rate per unit area $\Sigma_{\mathrm{SFR,disk}}$ varies approximately as

$$\Sigma_{\mathrm{SFR,disk}} = (2.5 \pm 0.7) \times 10^{-4} \left(\frac{\Sigma_{\mathrm{gas,disk}}}{M_\odot \mathrm{pc}^{-2}}\right)^{1.4\pm0.15} M_\odot\,\mathrm{kpc}^{-2}\mathrm{yr}^{-1} \tag{6.34}$$

$$\propto \Sigma^{1.4}_{\mathrm{gas,disk}}. \tag{6.35}$$

1.9 Initial Mass Function (IMF): Salpeter or Kroupa

According to single burst stellar population synthesis models, most of the stellar mass is lost at early times, before an age of ~ 2 Gyr: 25% and 36% of the total initial mass are lost for the Salpeter and Kroupa IMF, respectively. The approxmiated modelKim & Pellegrini (2012) is:

$$\dot{M}_\star(t) = 10^{-12}\,A \times \left(\frac{M_\star}{M_\odot}\right) t_{12}^{-1.3} \quad M_\odot \mathrm{yr}^{-1}, \tag{6.36}$$

where $M_\star$ is the galactic stellar mass at an age of 12 Gyr, t_{12} is the age in units of 12 Gyrs, and $A = 2.0$ or 3.3 for a Salpeter or Kroupa IMF.

Chapter 7

High Energy AstroPhysics

1 High Energy AstroPhysics

1.1 Schwarzschild radius

$$R_s = \frac{2GM}{c^2} \tag{7.1}$$

1.2 Eddington limits

For gas accretion - there is a maximum luminosity at which the environment of a black hole of M_{BH} may shine and still accrete gas, called Eddington limit, L_{Edd}. This limit is obtained by setting the outward continuum radiation pressure equal to the inward gravitational force. Denoting the gravitational potential with Φ, pressure with P, density with ρ,

$$\nabla\Phi = -\frac{\nabla P}{\rho} = \frac{\kappa}{c}F_{rad}, \tag{7.2}$$

where in the last equality we assumed that the pressure is dominated by radiation pressure which is associated to a radiation flux, F_{rad}. Here κ is the opacity. There are two primary sources of opacity for the typical densities and temperatures here: Thomson electron scattering and bremsstrahlung (i.e labeled free-free absorption) with

$$\kappa_{es} = \frac{\sigma_T}{m_p} = 0.4 \text{ cm}^2\text{g}^{-1}, \tag{7.3}$$

$$\kappa_{ff} \approx 8 \times 10^{22}\ \mathrm{cm^2 g^{-1}} \left(\frac{\rho}{\mathrm{g\,cm^{-3}}}\right) \left(\frac{T}{\mathrm{K}}\right)^{-7/2}, \tag{7.4}$$

where we assumed a pure hydrogen plasma for simplicity, where m_p denotes proton mass and σ_{T} denotes the Thomson cross section. For the definition of the luminosity,

$$L = \int_S F_{rad} \cdot dS = \frac{c}{\kappa} \int_S \nabla \cdot dS \tag{7.5}$$

Using Gauss's theorem, Poisson's equation $\nabla^2\Phi = 4\pi G\rho$, and the definition of the mass,

$$L_{Edd} = \frac{c}{\kappa} \int_V \nabla^2\Phi dV = \frac{4\pi Gc}{\kappa} \int_V \rho dV = \frac{4\pi GMc}{\kappa} = 1.3 \times 10^{44} \left(\frac{M_{BH}}{10^6 M_\odot}\right) \mathrm{erg\,s^{-1}} \tag{7.6}$$

1.3 SuperNova explosion & Remnant

SNR phases

There are 4 phases in the evolution of supernova remnants (SNRs): free-expansion, Sedov expansion, snowplow phase and relaxing phase. Fig. (7.1) shows the correlation between the size of bubble and the evolution time along the phases.

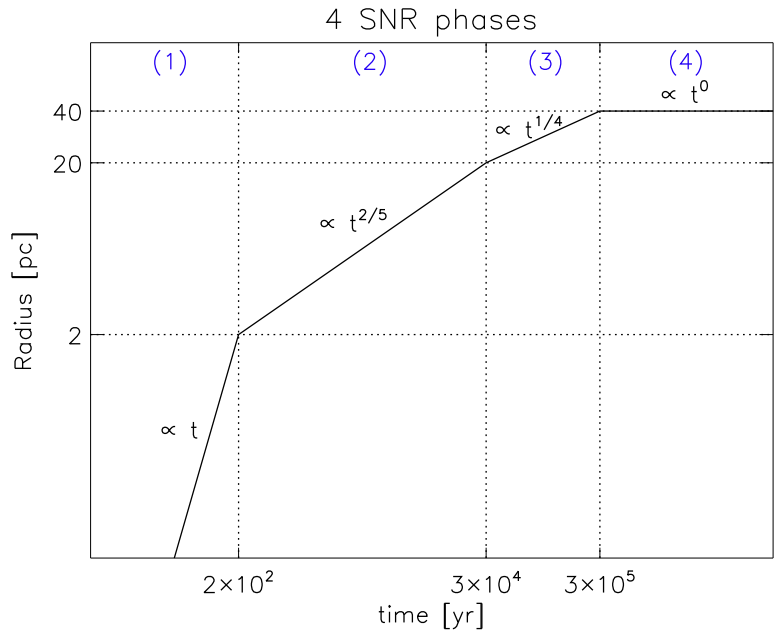

Figure 7.1 4 Supernova remnants phases: (1) free expansion (2) Sedov-Taylor expansion (3) Snowplow phase (4) relaxing phase. Note that x&y axes are in logarithmic scale.

(1) free expansion ($v = v_{\rm ej}$ =constant)

The energy of supernova explosion is roughly:

$$E_{\rm SN} \sim \frac{1}{2} M_{\rm ej} v_{\rm ej}^2, \tag{7.7}$$

where the ejected outflow velocity is,

$$v_{\rm ej} \sim 10^4 \, km/s \left(\frac{E_{\rm SN}}{10^{51} \, erg}\right)^{1/2} \left(\frac{M_{\rm ej}}{M_\odot}\right)^{-1/2}. \tag{7.8}$$

The mass of swept-up gas becomes

$$M_{\rm swept-up} \sim \frac{4\pi}{3} r^3 \rho_{\rm ISM}. \tag{7.9}$$

As a result, the bubble radius during this phase increases until $M_{\rm swept-up} \sim M_{\rm ej}$,

$$r \sim 2 \, pc \left(\frac{M_{\rm ej}}{M_\odot}\right)^{1/3} \left(\frac{\rho_{\rm ISM}}{10^{-24} \, g \, cm^{-3}}\right)^{-1/3}, \tag{7.10}$$

and the final time of this stage is

$$t \sim \frac{r}{v_{\rm ej}} \sim 200 \, yr \left(\frac{E_{\rm SN}}{10^{51} \, erg}\right)^{-1/2} \left(\frac{M_{\rm ej}}{M_\odot}\right)^{5/6} \left(\frac{\rho_{\rm ISM}}{10^{-24} \, g \, cm^{-3}}\right)^{-1/3}. \tag{7.11}$$

(2) Sedov-Taylor expansion ($E = E_{\rm SN}$ =constant)

The energy is conserved in this stage: $E_{\rm SN} \propto M v^2 \propto \rho_{\rm ISM} r^3 \dot{r}^2$, thereby

$$\begin{aligned} r^3 \left(\frac{dr}{dt}\right)^2 &\propto \frac{E_{\rm SN}}{\rho_{\rm ISM}} \\ r^{3/2} dr &\propto \left(\frac{E_{\rm SN}}{\rho_{\rm ISM}}\right)^{1/2} dt \\ \therefore r &\propto \left(\frac{E_{\rm SN}}{\rho_{\rm ISM}}\right)^{1/5} t^{2/5} \end{aligned} \tag{7.12}$$

The typical outflow velocity is $\sim 200 \, km/s$ and the temperature drops to $10^6 \, K$, which emits strong X-ray thermal bremsstrahlung.

(3) Snowplow phase (p=constant)

The temperature drops below $10^6\,K$ so that radiative cooling becomes dominant by some recombination processes. In this stage, the cold dense shell is driven by the hot interior.

$$\frac{d}{dt}(M\,v) = \frac{d}{dt}\left(\frac{4\pi}{3}\,\rho\,r^3\,\dot{r}\right) = 0. \tag{7.13}$$

Assuming a thin shell forms at t_0 with the size of r_0 and the outflow velocity of v_0,

$$\begin{aligned} r^3\,\dot{r} &= r_0^3\,v_0 \\ r &= r_0\left[1+\frac{4\,v_0(t-t_0)}{r_0}\right]^{1/4}. \end{aligned} \tag{7.14}$$

(4) mixing phase with ISM (r=constant)

The typical temperature and outflow velocity are $10^4\,K$ and $10\,km/s$, respectively. The speed of ejecta becomes comparable to the sound speed of ISM.

bubble with continuous energy injection: (bubble at pulsars or microquasars)

The solution for the expanding shock front supported by spin-down energy from central pulsar wind must be a scale-free or self-similar solution, which can be expressed of the dimensionless variable, η, where

$$\eta \equiv r\,t^l\,\rho_0^m\,\dot{E_0}^n, \tag{7.15}$$

the exponents l,m, and n are determined by the requirement that η is dimensionless. Since the $\dot{E}_0$ has the dimensionality $M\,L^2\,T^{-3}$, and the ρ_0 has the dimensionality $M\,L^{-3}$, the dimensionality of η should be $L^{1-3m+2n}\,T^{l-3n}\,M^{m+n}$. Therefore, the exponents $l = -3/5, m = 1/5$, and $n = -1/5$,

$$\eta = r\left(\frac{\rho_0}{\dot{E}_0 t^3}\right)^{1/5}, \tag{7.16}$$

or,

$$R_s(t) = \eta\left(\frac{\dot{E}_0}{\rho_0}\right)^{1/5} t^{3/5}. \tag{7.17}$$

In order to calculate the normalized factor, η, descriptions in Castor et al. (1975) are adopted. In their notation, region b indicates a hot, almost isobaric region consisting of shocked stellar wind, and region c indicates a thin, dense, cold shell at radius,R_s expending at velocity $\dot{R}_s$, and containing most of the swept-up ISM gas.

The dominant energy loss of region b is work against the dense shell, region c, so that the total energy of region b should be

$$\dot{E}_b = \dot{E}_0 - 4\pi R_s^2 P_b \dot{R}_s, \tag{7.18}$$

with

$$\frac{4}{3}\pi R_s^3 P_b = \frac{2}{3} E_b. \tag{7.19}$$

In addition, the motion of the shell, region c, follows from

$$\frac{d}{dt}\left[M_c(t)\dot{R}_s(t)\right] = 4\pi R_s^2 P_b, \tag{7.20}$$

where

$$M_c(t) = \frac{4}{3}\pi \rho_0 R_s^3, \tag{7.21}$$

assuming that most of the swept-up interstellar mass remains in the shell. Combining eq. (7.18)-(7.21) allows us to derive the radial evolution of the shell. As we differentiate eq. (7.19),

$$\dot{E}_b = 6\pi R_s^2 \dot{R}_s P_b + 2\pi R_s^3 \dot{P}_b, \tag{7.22}$$

and combine it with eq. (7.18),

$$\therefore\ 10\pi R_s^2 \dot{R}_s P_b + 2\pi R_s^3 \dot{P}_b = \dot{E}_0 \tag{7.23}$$

Meanwhile, eq. (7.20)&(7.21) can be further calculated as,

$$\begin{aligned} \frac{d}{dt}\left[\frac{4}{3}\pi R_s^3 \rho_0 \dot{R}_s\right] &= 4\pi R_s^2 P_b \\ \rightarrow 3\dot{R}_s^2 + R_s\ddot{R}_s &= 3\frac{P_b}{\rho_0}. \end{aligned} \tag{7.24}$$

For the purpose of simplification, we substitute $\eta\left(\frac{\dot{E}_0}{\rho_0}\right)^{1/5} \equiv A$, where A is constant, then we set eq. (7.17) to $R_s(t) = A\,t^{3/5}$. Plugging it into eq. (7.24) allows us to express P_b as,

$$P_b(t) = \frac{7}{25}A^2\,\rho_0\,t^{-4/5}, \tag{7.25}$$

Finally we plug eq. (7.25) into eq.(7.23), we get

$$\begin{aligned} \frac{154}{125}\pi A^5 \rho_0 &= \dot{E}_0 \\ \therefore A &= \left(\frac{\dot{E}}{\rho_0}\right)^{1/5}\left(\frac{125}{154\pi}\right)^{1/5} \end{aligned} \tag{7.26}$$

or equivalently,

$$\eta = \left(\frac{125}{154\pi}\right)^{1/5}. \tag{7.27}$$

1.4 Accretion Disk

overview

In the 1960s, X-ray observations and radio imaging of cosmic sources led to the realization that compact objects are a) numerous and b) extremely bright and c) extremely luminous. Understanding what powers these sources required the formulation of a theory of accretion.

Beyond high energy astrophysics, accretion is important in many other scenarios, such as star formation and growth of starcluster.

- Arguments for accretion onto compact objects:
  Consider a cosmic X-ray source (either an X-ray binary or an AGN).

  AGN: Observe $L_{bol} \approx 10^{45} - 10^{46}\ \mathrm{erg\,s^{-1}}$
  Observe variability with $\Delta\tau \sim$ hours $-$ years

  XRB: Observe $L_{bol} \approx 10^{38}\ \mathrm{erg\,s^{-1}}$
  Observe variability with $\Delta\tau \sim 10^{-3} - 1\,\mathrm{sec}$

- Causality: For a stationary object emitting with considerable variability on timescale $\Delta\tau$ (with ≥ 50 % ΔL), we infer a size unit of

$$R_{obj} \leq \Delta\tau \cdot c, \tag{7.28}$$

  from causality arguments (significant portion of the object must light up within $\Delta\tau$, and light travel time across object must, therefore, be $\leq \Delta\tau$)

  $\Rightarrow$ $\mathrm{R_{AGN}} \leq$ AU to PC

  $\mathrm{R_{XRB}} \leq$ 100 km to $\mathrm{R_\odot}$

- Efficiency: Suppose the object is powered by consuming some fuel at some rate $\dot{M}$ and converting to radiation with some efficiency η:

$$L = \eta \dot{M} c^2, \tag{7.29}$$

  so,

$$\begin{aligned} \dot{M} = \frac{L}{\eta c^2} &= 1.4 \times 10^{18}\,\mathrm{g\,s^{-1}} \left(\frac{L}{10^{38}\,\mathrm{erg\,s^{-1}}}\right)\left(\frac{10\%}{\eta}\right) \\ &\cong 2 \times 10^{-8}\,\mathrm{M_\odot\,yr^{-1}} \left(\frac{L}{10^{38}\,\mathrm{erg\,s^{-1}}}\right)\left(\frac{10\%}{\eta}\right) \end{aligned} \tag{7.30}$$

- Characteristic masses: Dynamical mass estimates are available for both AGN and XRBs

$$\left.\begin{array}{ll} M_{AGN} & \sim 10^6 - 10^{10}\,M_\odot \\ M_{XRB} & \sim 1 - 30\,M_\odot \end{array}\right\} \textbf{Compact Object !}$$

- Possible power sources:

  a) Chemical: $\eta_{chem} \approx$ eV/nucleon $\approx 10^{-9}$

b) Nuclear: $\eta_{nuc} \approx$ MeV/nucleon $\approx 10^{-3}$

c) accretion:

$$\begin{aligned} R_{isco} &= \frac{6GM}{c^2} \\ \Delta E_{isco} &= \frac{1}{2}\frac{GMm_p}{R_{isco}} = \frac{GMm_pc^2}{12GM} = \frac{m_pc^2}{12} \\ \rightarrow \eta_{acc} &\approx \frac{1}{12} \approx 10\,\% \approx 100 \times \eta_{nuc} \approx 10^8 \eta_{chem} \end{aligned}$$

accretion by far the most efficient power source.

- Growth time:

$$T_{\dot{M}} = \frac{M}{\dot{M}} = 4 \times 10^7\, yrs \left(\frac{\eta}{10\%}\right)\left(\frac{M}{M_\odot}\right)\left(\frac{10^{38}\, erg\, s^{-1}}{L}\right) \tag{7.31}$$

This immediately rules out chemical power and even a nuclear powered source with quickly run out of fuel. We will formalize this argument further in the context of AGN.

How does accretion work?

Spherical/Bondi-Hoyle accretion:
Consider massive, gravitating compact object placed in a stationary, uniform medium

$\Rightarrow$ no pressure gradients to support against gravity.

$\Rightarrow$ spherically symmetric infall (no preferred direction)

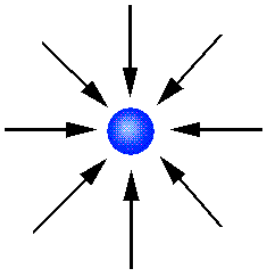

Figure 7.2 sketch of spherical infall

Questions:

- What is the structure of such a flow?
- How much gas is accreted at what rate?
- How much energy is released?

- what is the applicability of such a solution?

Order of magnitude estimates:

The event horizon for a black hole is $2\frac{GM}{c^2} \equiv r_s$. Inside r_s, even light, moving at c, is bound and must travel inward, the region inside is causally disconnected. Regular matter is bound to black hole further out: For material with temperature T and sound speed $c_s \approx \sqrt{kt/m_p}$, material is bound for

$$\begin{aligned} E_{thermal} &\leq E_{pot} \\ \Leftrightarrow\ kT = m_p c_s^2 &\leq \frac{GMm_p}{r_{Bondi}} \end{aligned} \tag{7.32}$$

$$\therefore r_{Bondi} \sim \frac{GM}{c_s^2} \tag{7.33}$$

,Bondi radius, is the capture radius of the black hole for gas at temperature T. Inside r_{Bondi}, gas must be bound to the black hole.

Spherical accretion: no hydrostatic pressure support

$\Rightarrow \quad v_{Bondi} \approx -c_s$

At r_{Bondi}, so for gas with density ρ, accretion rate is

$$\begin{aligned} \dot{M} &\approx 4\pi R^2 \rho v = 4\pi r_{Bondi}^2 \rho c_s \\ &= \frac{4\pi G^2 M^2 \rho}{c_s^3} \end{aligned} \tag{7.34}$$

Note: $\dot{M} \propto M^2$ and $\dot{M} \propto c_s^{-3} \propto T^{-3/2}$.

a) Stellar mass compact object:

$$\dot{M}_{Bondi} \approx 5 \times 10^{11}\, g\, s^{-1} \left(\frac{M}{M_\odot}\right)^2 \left(\frac{n_{ISM}}{1\, cm^{-3}}\right) \left(\frac{T}{10^4\, K}\right)^{-3/2} \tag{7.35}$$

For accretion at 10% efficiency, luminosity is

$$L_{Bondi} \approx 10^{31}\, \mathrm{erg\, s^{-1}} \tag{7.36}$$

b) Supermassive black holes:

$$\begin{aligned} \dot{M}_{Bondi} &\approx 5 \times 10^{23} \mathrm{g\,s^{-1}} \left(\frac{M}{3 \times 10^9\, M_\odot}\right)^2 \left(\frac{n}{10^{-2}\, cm^{-3}}\right) \left(\frac{c_s}{400\,\mathrm{km\,s^{-1}}}\right)^{-3} \\ &\approx 2.5 \times 10^{-10}\,\mathrm{M_\odot\,s^{-1}} \approx 0.03\,\mathrm{M_\odot\,yr^{-1}} \end{aligned} \tag{7.37}$$

and again for 10% efficiency:

$$L_{Bondi} \approx 5 \times 10^{43} \mathrm{erg\,s^{-1}} \left(\frac{M}{M_{87}}\right)^2 \left(\frac{n}{10^{-2}\, cm^{-3}}\right) \left(\frac{c_s}{400\,\mathrm{km\,s^{-1}}}\right)^{-3} \tag{7.38}$$

$\Rightarrow$ Bondi accretion might be sufficient for moderate AGN powers, it never works to power XRBs. That's why we can't see isolated black holes of stellar mass inside our Galaxy, even if they exist.

$\therefore$ Need another source of matter for XRBs.

Detailed solution of Bondi-Hoyle accretion

Problems with spherical accretion:

a) Radiation pressure
The radiative force on a particle is

$$\begin{aligned} F_{rad} &= \text{radiation momentum flux} \times \text{cross section} \\ &= \int d\nu \frac{F_\nu}{c} \sigma_\nu \end{aligned} \tag{7.39}$$

For ionized gas, use σ_T and $F = L/4\pi r^2$.

Radiation pressure becomes overwhelming when the radiative force exceeds the gravitational force:

$$F_{rad} = \frac{L}{4\pi r^2} \frac{\sigma_T}{c} > \frac{GM}{r^2} m_p \tag{7.40}$$

$$\Leftrightarrow \boxed{L > L_{\mathrm{Edd}} = \frac{GMm_p 4\pi c}{\sigma_T} = 1.3 \times 10^{38}\,\mathrm{erg\,s^{-1}} \left(\frac{M}{M_\odot}\right)} \tag{7.41}$$

where L_{Edd} is Eddington Luminosity. Note that L_{Edd} is independent of r and can be higher for non-ionized, heavy particles.

For an accretion efficiency of 10%, L_{Edd} corresponds to an accretion rate of

$$\begin{aligned} \dot{M}_{Edd} &= \frac{L_{Edd}}{0.1\,c^2} \\ &= 1.4\times10^{18}\,\mathrm{g\,s^{-1}}\,M/M_\odot = 2\times10^{-8}\,\mathrm{M_\odot\,yr^{-1}}\,M/\mathrm{M_\odot} \end{aligned} \tag{7.42}$$

b) Angular momentum

The assumption of spherical symmetry is almost always incorrect: any realistic gas reservoir will have net angular momentum with respect to accreting object.

⇒ centrifugal barrier prevents radial infall

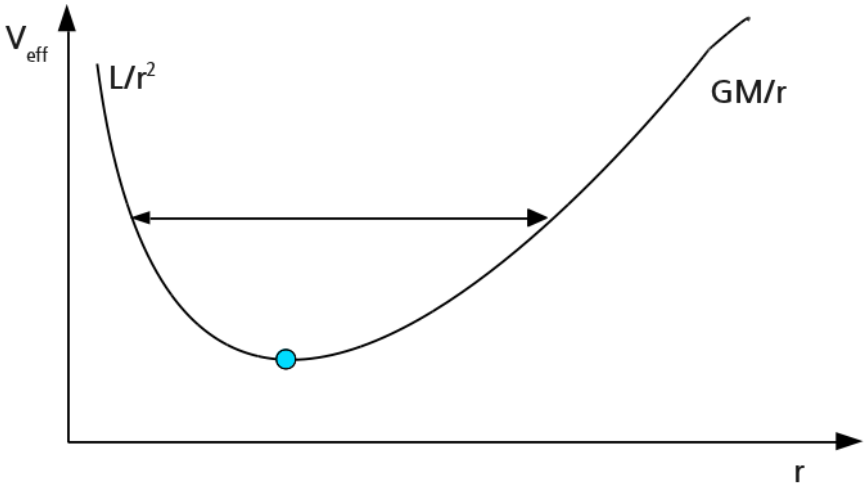

Figure 7.3 Effective energy with angular momentum, L. Circular orbit will be taken at minimum energy for given L.

⇒ Crossing eccentric orbits dissipate and circularize.

No centrifugal barrier in vertical direction to counteract z-component of gravity: **disk formation**

Vertical hydrostatic balance:

⇒ Only pressure gradient balances vertical gravity.

$$r\Omega = v_\phi \tag{7.43}$$

$$r\Omega^2 = \frac{GM}{r^2} \tag{7.44}$$

$$(\text{cf. } L = r^2\Omega = r^2\sqrt{\frac{GM}{r^3}} \propto r^{1/2} \text{ for keplerian disk}) \tag{7.45}$$

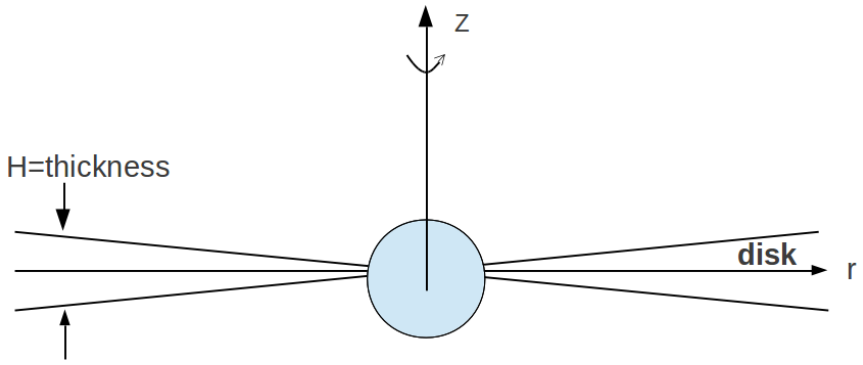

Figure 7.4 Sketch of accretion disk. Centered object will be black hole or neutron star, ... $F_z \cong \frac{GM}{r^2}\frac{z}{r}$

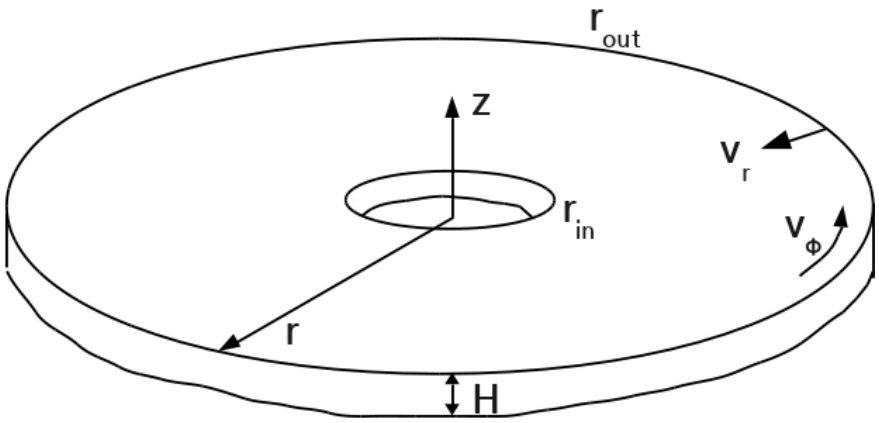

Figure 7.5 Hydrostatic balance in accretion disk.

The pressure gradient in vertical direction will be balanced by the gravity via

$$\nabla_z P = \frac{\partial}{\partial z} P = \rho g_z = -\frac{GM\rho}{r^2}\frac{z}{r} = -\rho\Omega^2 z \tag{7.46}$$

Ansatz: $H \ll r$ and $v_r \ll v_\phi$.

$$\Rightarrow \quad \frac{\partial P}{\partial z} \approx -\frac{P}{H} = -\rho\Omega^2 z \approx -\rho\Omega^2 H \tag{7.47}$$

$$\Leftrightarrow \quad \frac{P}{\rho} \approx \Omega^2 H^2 = R^2\Omega^2\left(\frac{H^2}{R^2}\right) = v_\phi^2\left(\frac{H}{R}\right)^2 \tag{7.48}$$

$$\Leftrightarrow \boxed{\left(\frac{c_s^2}{v_\phi^2}\right) \approx \left(\frac{H}{R}\right)^2} \tag{7.49}$$

$$\Rightarrow \; v_\phi \gg c_s \;\Leftrightarrow\; r \gg H \tag{7.50}$$

Note that assumption of this model is 1) steady state ($\partial/\partial t = 0$), 2) $r \gg H$,and 3) $v_\phi \gg v_r$.

$\therefore$ Thin accretion disks ($H \ll r$) must be cold ($c_s \ll v_\phi$).

Also note that a virialized flow would have $c_s \approx v_\phi$.

Order of Magnitude Scaling:

a) Mass conservation:

From continuity equation (eq.(2.4)), mass transfer rate can be roughly estimated as

$$\dot{M} = -2\pi R\, H\rho\, v_R \equiv -2\pi R\, \Sigma\, v_R, \tag{7.51}$$

where Σ is surface density. The factor 2 in the equation can be derived by second term in eq.(2.4).

$$\Rightarrow \boxed{\dot{M} \propto R\, \Sigma\, v_R} \tag{7.52}$$

b) Vertical hydrostatic balance:

From the relation ship in eq.(7.48),

$$\Rightarrow \; \frac{P}{\rho} \sim c_s^2 \propto \Omega^2 H^2 \propto v_\phi^2 \left(\frac{H}{R}\right)^2 \tag{7.53}$$

$$\Rightarrow \boxed{T \propto \Omega^2 H^2} \tag{7.54}$$

where T is gas pressure dominated temperature in the accretion disk.

c) Angular momentum conservation:

Advection will be produced by torque

$$\dot{M}R^2\Omega \approx \underbrace{2\pi R\,H}\cdot\underbrace{R}\cdot\underbrace{\rho\nu\frac{\partial\Omega}{\partial R}R} \tag{7.55}$$

where LHS is given by derivation of angular momentum, $\partial L/\partial t = \partial(M\,R^2\Omega)/\partial t$, and in RHS, first term is surface area and second term is lever arm and third term is viscous stress. The angular momentum will be transported to outward by viscosity.

$$\therefore\ \boxed{\dot{M} \propto \Sigma\,\nu} \tag{7.56}$$

d) Energy conservation:

Sources = Sinks $(Q^+ = Q^-)$

Here sources can be gravity and the sinks can be radiation, advection(neglect for now).

$$Q^+ \sim \frac{d\,E_{pot}}{dt\,dR}dR \sim \frac{GM\dot{M}}{R^2}dR \tag{7.57}$$

$$Q^- \sim 2\pi R\,dR\cdot F \sim 2\pi R\,dR\cdot\sigma T_{eff}^4 \tag{7.58}$$

Under the cool disk assumption, the flux will be dominant for blackbody radiation due to high opacity.

$$\Rightarrow\ T_{eff}^4 \propto \frac{GM\dot{M}}{R^3} \propto \Omega^2\dot{M} \propto M\dot{M}R^{-3} \tag{7.59}$$

Interested in T_{central}: Optically thick radiation Radiation escapes from $\tau \leq 1$

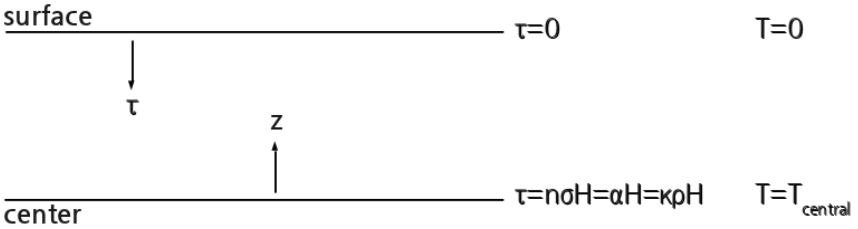

Figure 7.6 Sketch of optical depth through disk

$$\Rightarrow\ T_{\text{eff}}^4 \approx T_{\tau=1}^4 \approx \frac{dT^4}{d\tau}\tau_{=1} \approx \frac{4T_{central}^4}{\tau_{central}} \approx \frac{4T_c^4}{\kappa\rho H} \tag{7.60}$$

$$\therefore \boxed{\frac{T_c^4}{\kappa\rho H} \propto \Omega^2 \dot{M}} \tag{7.61}$$

Note that $\rho H = \Sigma$, so $T_c^4 \propto \kappa\Sigma\Omega^2\dot{M}$.

And we will use Kramer's opacity, which is blackbody-weighted absorption.

$$\boxed{\kappa_{kr} \propto \rho T^{-7/2} \propto \frac{\Sigma}{H} T^{-7/2}} \tag{7.62}$$

e) Viscosity: ν

- Describe microscopic transport of momentum
- Characterized by typical transport velocity $\tilde{v}$ and typical random step size λ:

$$\nu \approx \lambda \tilde{v} \tag{7.63}$$

- Molecular viscosity (kinetic theory):

$$\nu \approx \lambda_{mfp} c_s \tag{7.64}$$

where λ_{mfp} is characteristic length of mean free path.

For astrophysical systems of size l, often $\lambda_{mfp} \ll l$

$$\Rightarrow \text{Re} \equiv \frac{\text{inertial transport}}{\text{viscous transport}} = \frac{l\, v}{\lambda_{mfp} c_s} \gg 1 \tag{7.65}$$

where Re is the Reynolds number.

$\Rightarrow$ **Turbulence !!!!!**

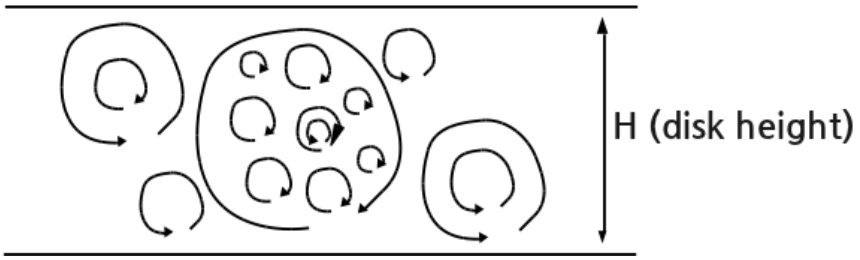

Figure 7.7 Eddies in the accretion disk. Characteristic length scale is maximum eddie size ($l \approx$ H).

- Characteristic speed: sound speed, $\tilde{v} \approx c_s$.

$$\therefore \quad \boxed{\nu \equiv \alpha c_s H, \quad \alpha \leq 1} \tag{7.66}$$

  Which is α**-disk model**.

- viscosity continued:
  α contains all uncertainties about ν very likely smaller than unity ($\alpha \leq 1$). Very convenient, but ...

Putting it all together:

$$\begin{array}{lll}
(1) & \dot{M} \sim R\Sigma v_R & (\text{mass conservation}) \\
(2) & H \sim T^{1/2}\Omega^{-1} & (\text{vertical structure}) \\
(3) & \nu \sim \alpha T^{1/2} H & (\text{ff} - \text{viscosity}) \\
(4) & \dot{M} \sim \Sigma\nu \sim \Sigma\alpha T^{1/2} H & (\text{angular momentum}) \\
(5) & \frac{T^4}{\kappa\Sigma} \sim \dot{M}\Omega^2 & (\text{energy equation}) \\
(6) & \kappa \sim \Sigma\, T^{-7/2} H^{-1} & (\text{Kramer's opacity})
\end{array}$$

Solutions:

$$\boxed{T \sim \dot{M}^{3/10}\alpha^{-1/5}M^{1/4}R^{-3/4}} \tag{7.67}$$

$$\boxed{\Sigma \sim \dot{M}^{7/10}\alpha^{-4/5}M^{1/4}R^{-3/4}} \tag{7.68}$$

$$\boxed{v_R \sim \dot{M}^{3/10}\alpha^{4/5}M^{-1/4}R^{-1/4}} \tag{7.69}$$

where in the steps, we have used $\Omega \sim M^{1/2}R^{-3/2}$.

Conclusions:

1) α enters T only marginally.

2) $v_R \sim R^{-1/4}$ but $c_s \sim R^{-3/8}$
   $\Rightarrow$ $\frac{v_R}{c_s} \equiv M \sim R^{1/8}$
   $\Rightarrow$ less and less supersonic at smaller radius

3) $v_R \sim \alpha^{4/5}$
   $\Rightarrow$ advection becomes more important for large α.

A complete algebraic solution gives:

$$T_c = 1.4 \times 10^4\, K\, \alpha^{-1/5} \dot{M}_{16}^{3/10} M^{1/4} R_{10}^{-3/4} f^{6/5} \tag{7.70}$$
$$v_R = 2.7 \times 10^4\, cm\, s^{-1}\, \alpha^{4/5} \dot{M}_{16}^{3/10} M^{-1/4} R_{10}^{-1/4} f^{-14/5} \tag{7.71}$$
$$\tau = 33\, \alpha^{-4/5} \dot{M}_{16}^{1/5} f^{4/5} \tag{7.72}$$
$$H = 1.7 \times 10^8\, cm\, \alpha^{-1/10} \dot{M}_{16}^{3/20} M^{-3/8} R_{10}^{9/8} f^{3/5} \tag{7.73}$$
$$\Sigma = 5.2\, g\, cm^{-2}\, \alpha^{-4/5} \dot{M}_{16}^{7/10} M^{1/4} R_{10}^{-3/4} f^{14/5} \tag{7.74}$$

with $\dot{M}_{16} = \dot{M}/10^{16}\, g\, s^{-1}$, $M = M_{BH}/M_\odot$, $R_{10} = R/10^{10}\, cm$,
and $f = \left[1 - \beta\,(R_i/R)^{1/2}\right]^{1/4}$ where β is a viscous coupling constant.
Note that $T_{\rm eff}^4 \sim \Omega^2 \dot{M} \sim M\dot{M}R^{-3}$, that is independent of α!!

Spectrum:

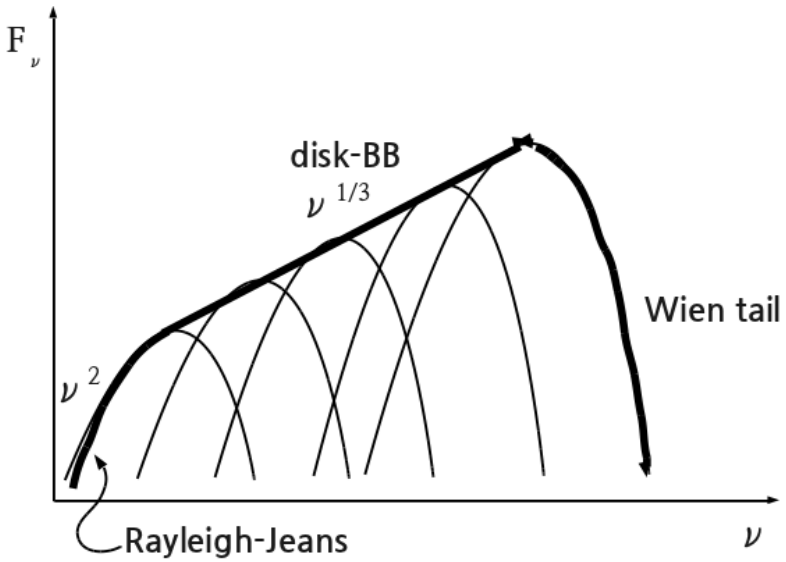

Figure 7.8 spectrum from accretion disk

The black body spectra from each part of accretion disk are superposed to produce characteristic spectrum. The higher peak frequency of overlaid spectrum comes from inner disk.

$$T_{\rm eff} = 1.3 \times 10^7\, K\, \dot{M}_{17}^{1/4} M^{1/4} R_6^{-3/4} \quad \text{(neutron star)}$$
$$T_{\rm eff} = 1.3 \times 10^5\, K\, \dot{M}_{25}^{1/4} M_8^{1/4} R_{14}^{-3/4} \quad (10^8\, \mathrm{M}_\odot \text{ black hole})$$

The role of magnetic fields: The magneto-rotational instability

a) The exact nature of the agent of angular momentum transport was unspecified (hidden in the α-parameter)

$\Rightarrow$ Magnetic stresses could be responsible:

A field line anchored into a ring at radius r will co-rotate with this ring. It will try to speed up ring r_+(outer ring) and slow down ring r_-(inner ring).

$\Rightarrow$ angular momentum transport

From MHD: magnitude of magnetic stress is $\frac{(\vec{B}\cdot\nabla)\vec{B}}{4\pi}$.

Question: is $\frac{(\vec{B}\cdot\nabla)\vec{B}}{4\pi}$ sufficient, *i.e.* , is B-field large enough?

Answer: It will be, after a few Keplerian orbits.

b) **Magneto-rotational instability (MRI):**

Consider a vertical field line with a radial perturbation (fig.(7.9)).

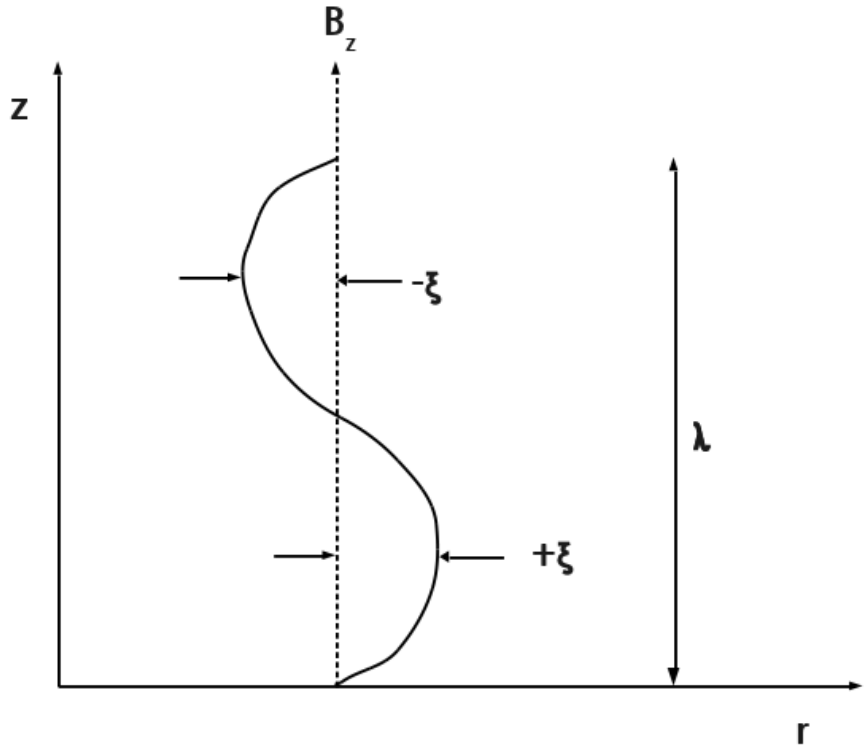

Figure 7.9 Vertical magnetic field line

Here, wavelength $\lambda \leq$ H and amplitude(linear regime) $\xi \ll \lambda$.

Magnetic force density in radial direction is (comment: $B_r \sim B_z \cdot \frac{\xi}{\lambda}$

$$f_B = \frac{B_z}{4\pi}\frac{\partial}{\partial z}B_r \sim \frac{B_z}{4\pi}\left(-\frac{B_r}{\lambda}\right) \sim \frac{B_z^2}{4\pi}\left(-\frac{\xi}{\lambda^2}\right) \propto -\left(\vec{k}\cdot\vec{v}_A\right)^2 \rho\,\xi \tag{7.75}$$

where v_A is the Alfv́en speed, $v_A^2 = \frac{B_z^2}{4\pi\rho}$.

The net centrifugal force resulting from the perturbation is

$$f_c = -\rho R \frac{\partial}{\partial R}(\Omega^2)\xi = -\rho \frac{d\Omega^2}{d\,lnR}\xi \tag{7.76}$$

The centrifugal force excess wins if

$$f_c + f_B = -\rho \left(\frac{d\Omega^2}{d\,lnR} + \left(\vec{k}\cdot\vec{v}_A\right)^2 \right) \xi \quad (> 0 \text{ for instability}) \tag{7.77}$$

which is positive for

$$\frac{d\Omega^2}{d\,lnR} < -\left(\vec{k}\cdot\vec{v}_A\right)^2 \quad \Rightarrow \text{ instability} \tag{7.78}$$

So there is a minimum wavelength (maximum k) for which the instability grows and we need

$$\frac{d\Omega^2}{dR} < 0 \tag{7.79}$$

with $\frac{B_z^2}{\lambda_z^2\rho} \leq \Omega^2$ or $\lambda_z^2 \geq \frac{B_z^2}{\Omega^2\rho}$. So unstable as long as H $\geq \lambda_{\min}$ or B $\leq$ equipartition. (because $B^2 \leq \mathrm{H}^2\Omega^2\rho \leq P$, where $\mathrm{H}^2\Omega^2 = c_s^2$ in equipartition).

Other accretion regimes

We have neglected (among other things):

- the inner boundary
- radiation pressure
- advection of energy
- time dependence
- non-local dissipation (B-fields), *i.e.* , magnetic reconnection

a) Radiation pressure:

$$P_{\text{thermal}} \propto T \quad vs. \quad P_{rad} \propto T^4 \tag{7.80}$$

Since, for the standard thin disk $T \sim \dot{M}^{3/10}\alpha^{-1/5}M^{1/4}R^{-3/4}$, the radiation pressure must dominate at large $\dot{M}$, small R.

It is straight forward to re-do the analysis by replacing the pressure term $\frac{aT^4}{3}$, but hardly worth is:

Radiation pressure supported disks are thermally and viscously unstable.

$\Rightarrow$ equilibrium solution is never established.

Note: an accretion disk is anisotropic, so in principle, it can exceed the Eddington limit by a factor of a few.

b) **Advection Dominated Accretion Flows (ADAFs)**

We have neglected energy advection Q^-_{Adv} in the energy balance. The advective term becomes important in (a) high $\dot{M}$ cases, where it can alleviate the Eddington limit and (b) low $\dot{M}$, high α cases.

Advection always decreases the radiative efficiency of the flow.

Advection dominated solution:

$$Q^-_{Adv} \sim \Sigma T 2\pi R v_R \sim T\dot{M} \tag{7.81}$$

$$Q^+_{Adv} \sim \frac{GM\dot{M}}{R} \tag{7.82}$$

Balance:

$$T \sim \frac{GM}{R} \sim \Omega^2 R^2 \sim T_{virial} \quad \text{(hot)} \tag{7.83}$$

and with vertical hydrostatic balance: $T \sim \Omega^2 H^2$

$$H \sim T^{1/2}\Omega^{-1} \sim R \quad (\text{thick disk} \ \ (\text{cf. thin} \ \leftarrow \ \text{radiative dominate})) \tag{7.84}$$

so

$$v_R \sim \frac{\dot{M}}{\Sigma R} \tag{7.85}$$

and

$$\dot{M} \sim \Sigma\nu \sim \Sigma\alpha T^{1/2} H \tag{7.86}$$

$$\begin{aligned} \Rightarrow \quad v_R &\sim \frac{\dot{M}}{\Sigma R} \sim \frac{\Sigma\alpha T^{1/2} H}{\Sigma R} \sim \alpha T^{1/2} H/R \\ &\sim \alpha\Omega R \sim \alpha v_\phi \qquad \text{(rapid inflow)} \end{aligned} \tag{7.87}$$

Thus: Advection Dominated Accretion Flows are

- hot (roughly at Virial temperature), $T \sim T_{\rm vir}$
- thick (not so much disk-like, more spherical), H $\sim$ R
- non-Keplerian (radial velocity comparable to v_ϕ)
- require large α

Note: ADAFs require radiative losses to be inefficient.

In a hot flow, it is possible that ions and electrons are thermally decoupled. If the ions get heated, they might not transfer their energy to the electrons, who do all the radiating

$\Rightarrow$ Very hot flow implies strong Compton emission

$\Rightarrow$ Power-law emission (low-hard state ?)

As of today, it is not clear whether electrons and ions are really that strongly decoupled.

c) The inner boundary:
We have neglected entirely what happens at the inner boundary. Introduces correction $\vartheta(r_i/r)$...

i) Neutron stars; WDs:

Boundary layer must spin incoming material up or down to co-rotate with NS $\Rightarrow$ dissipation.

Residual kinetic and thermal energy must be dissipated and radiated (*i.e.* , no true advection).

ii) Black holes:

Usual assumption: zero-torque at marginally stable circular orbit (still introduces correction of order r_i/r to solution)

Energy can be advected across horizon.

$\Rightarrow$ are low luminosity sources advection dominant?

$\Rightarrow$ are black holes in quiescence dimmer than NS in quiescence because they have an event horizon?

But note: **"The absence of evidence is not the evidence of absence.**

In other words, black holes could be dim for other reasons, their dimness is no proof for the existence of event horizons (sadly, some might say)

d) Typical time scales

1) Signal propagation:

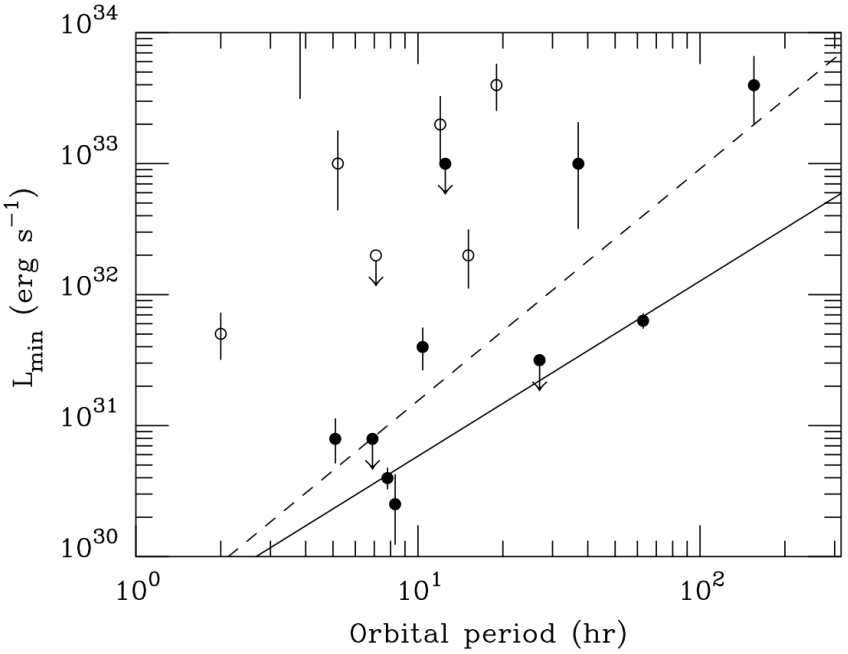

Figure 7.10 XRBs in quiescence (Hameury et al. 2003). Open circles represent neutron stars and filled circles represent black holes.

$$\begin{aligned} \tau_{visc} &\sim \frac{M}{\dot{M}} \sim \rho \frac{R^2 H}{\Sigma \nu} \sim \frac{\Sigma R^2}{\Sigma \nu} \\ &\sim \frac{R^2}{\nu} \approx 5 \times 10^5 \; R_{10}^{10/8} M^{2/8} \, \dot{M}_{16}^{-3/10} \alpha^{-4/5} \end{aligned} \tag{7.88}$$

Recall: ν has units length^2/time.

τ_{visc} is the time it takes for the disk to be drained completely if the accretion source turns off (*e.g.* , mass transfer from companion star)

2) Thermal (Kelvin-Helmholtz) time:

$$\begin{aligned} \tau_{th} &\sim \frac{E_{th}}{\dot{E}} \sim \frac{\rho c_s^2 R^2 H}{GM\dot{M}/R} \sim \frac{\Sigma c_s^2 R^3}{CM\Sigma\nu} \\ &\sim \frac{\Sigma c_s^2}{\Sigma \nu \Omega^2} \sim \frac{c_s^2 R^2}{\nu R^2 \Omega^2} \sim \frac{c_s^2 R^2}{\nu v_\phi^2} \end{aligned} \tag{7.89}$$

$$\therefore \tau_{th} \sim \tau_{visc} \left(\frac{c_s^2}{v_\phi^2} \right) \ll \tau_{visc} \tag{7.90}$$

⇒ Thermal evolution much more rapid than viscous for thin disks.

e) Non-local dissipation - corona

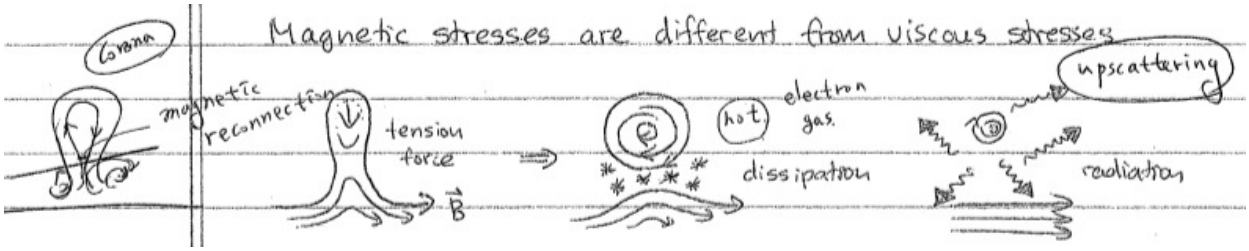

Figure 7.11 Magnetic stresses are different from viscous stresses

If viscosity is magnetic, dissipation will be dominated by reconnection.

⇒ Dissipation independent of ρ, field lines can rise out of disk and dissipate.

⇒ A layer of hot, low density gas will form above the disk - a "coronae" (See the Sun)

Emission: Soft photons from disk are Compton-upscattered (See fig.(7.12))

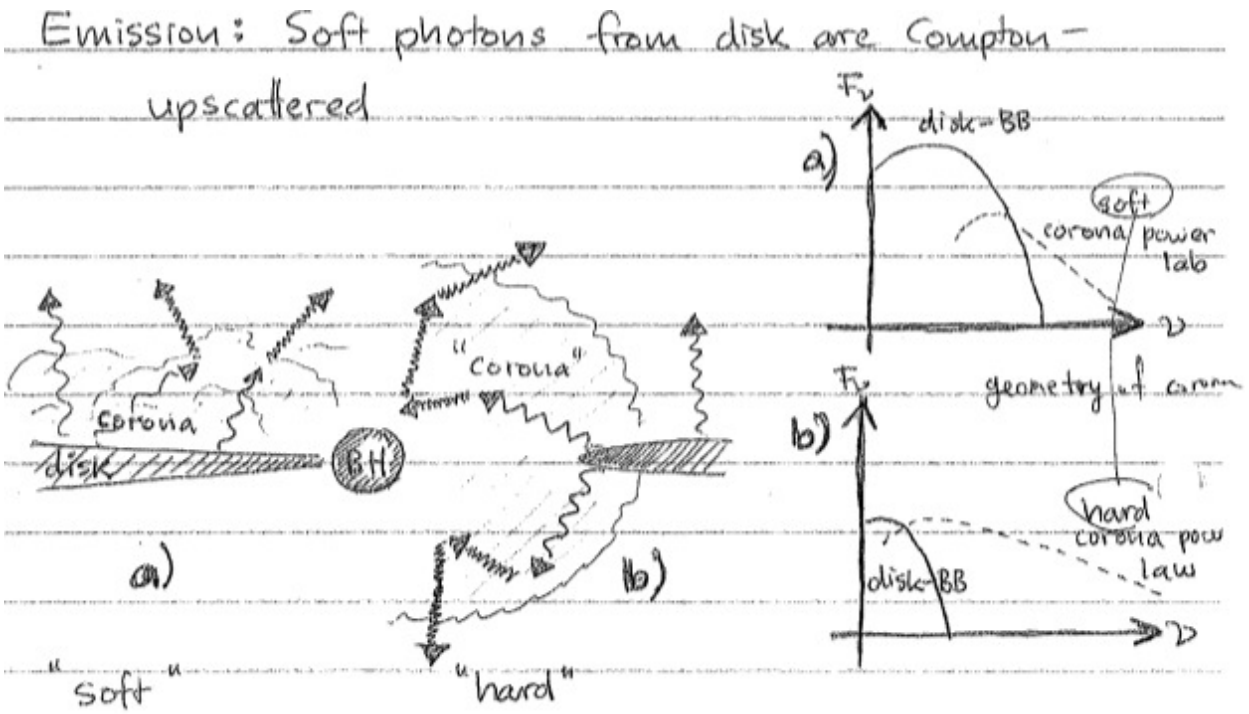

Figure 7.12 Emission: Soft photons from disk are Compton-upscattered

Viscosity Shear Stress: Spherical Coordinate

The tensors are working on both the momentum equation for angular momentum transport and the energy equation for viscous heating Stone et al. (1999):

$$\rho \frac{d\vec{v}}{dt} = -\nabla P - \rho \nabla \Phi + \nabla \cdot \boldsymbol{T} \tag{7.91}$$

$$\rho \frac{d(e/\rho)}{dt} = -P\nabla \cdot \vec{v} + \boldsymbol{T}^2/\mu \tag{7.92}$$

where $\boldsymbol{T}$ is an anomalous stress tensor, and $\mu = \rho\nu$ is the coefficient of shear viscosity, and ν is the kinematic viscosity coefficient:

$$\nu = \frac{\alpha\, c_s^2}{\Omega_{\rm k}} \tag{7.93}$$

where c_s is the sound speed of the medium, α is a conventional parameter for thin disk model by shakura & sunyaev (1973). and $\Omega_{\rm k}$ is the keplerian angular velocity,

$$\Omega_{\rm k} = \left(\frac{1}{r}\frac{\partial \Phi}{\partial r}\right)^{1/2}, \tag{7.94}$$

In spherical coordinates, the shear stress elements can be expressed as:

$$\boldsymbol{T}_{r\theta} = \boldsymbol{T}_{\theta r} = \mu \left\{ r\frac{\partial}{\partial r}\left(\frac{v_\theta}{r}\right) + \frac{1}{r}\frac{\partial v_r}{\partial \theta} \right\} \tag{7.95}$$

$$\boldsymbol{T}_{r\phi} = \boldsymbol{T}_{\phi r} = \mu \left\{ r\frac{\partial}{\partial r}\left(\frac{v_\phi}{r}\right) + \frac{1}{r\sin\theta}\frac{\partial v_r}{\partial \phi} \right\} \tag{7.96}$$

$$\boldsymbol{T}_{\theta\phi} = \boldsymbol{T}_{\phi\theta} = \mu \left\{ \frac{\sin\theta}{r}\frac{\partial}{\partial \theta}\left(\frac{v_\phi}{\sin\theta}\right) + \frac{1}{r\sin\theta}\frac{\partial v_\theta}{\partial \phi} \right\} \tag{7.97}$$

These derived tensors were confirmed by Okuda et al. (1997) (note that there are some typos in the equations of the paper). Since we are considering 2-D simulation (r, θ), $\partial/\partial\phi$ term in the equations above can be neglected.

The divergence of a tensor is

$$\nabla \cdot \boldsymbol{T} = \frac{\partial T_{ij}}{\partial x_j}\, \boldsymbol{e}_i. \tag{7.98}$$

Using this tensor calculus, the tensor term in eq. (7.91) can be expressed as

$$\begin{aligned}\nabla \cdot \boldsymbol{T} = &\left\{ \frac{\partial T_{rr}}{\partial r} + \frac{1}{r}\frac{\partial T_{r\theta}}{\partial \theta} + \frac{1}{r\sin\theta}\frac{\partial T_{r\phi}}{\partial \phi} + \frac{2\,T_{rr} + \cot\theta\, T_{r\theta} - T_{\theta\theta} - T_{\phi\phi}}{r} \right\} \hat{r} \\ &+ \left\{ \frac{\partial T_{\theta r}}{\partial r} + \frac{1}{r}\frac{\partial T_{\theta\theta}}{\partial \theta} + \frac{1}{r\sin\theta}\frac{\partial T_{\theta\phi}}{\partial \phi} + \frac{T_{r\theta} + 2T_{\theta r} + \cot\theta(T_{\theta\theta} - T_{\phi\phi})}{r} \right\} \hat{\theta} \\ &+ \left\{ \frac{\partial T_{\phi r}}{\partial r} + \frac{1}{r}\frac{\partial T_{\phi\theta}}{\partial \theta} + \frac{1}{r\sin\theta}\frac{\partial T_{\phi\phi}}{\partial \phi} + \frac{T_{r\phi} + 2T_{\phi r} + \cot\theta(T_{\theta\phi} + T_{\phi\theta})}{r} \right\} \hat{\phi}.\end{aligned} \tag{7.99}$$

Applying $T_{r\theta} = T_{\theta r}$, $T_{r\phi} = T_{\phi r}$, $T_{\theta\phi} = T_{\phi\theta}$ and ignoring normal stress terms and $\partial/\partial\phi$ terms, the eq. (7.99) can be rewritten as

$$\begin{aligned}\nabla \cdot \boldsymbol{T} = &\left\{ \frac{1}{r}\frac{\partial T_{r\theta}}{\partial \theta} + \frac{\cot\theta\, T_{r\theta}}{r} \right\} \hat{r} \\ &+ \left\{ \frac{\partial T_{r\theta}}{\partial r} + \frac{3\,T_{r\theta})}{r} \right\} \hat{\theta} \\ &+ \left\{ \frac{\partial T_{r\phi}}{\partial r} + \frac{1}{r}\frac{\partial T_{\theta\phi}}{\partial \theta} + \frac{3\,T_{r\phi} + 2\,\cot\theta\, T_{\theta\phi}}{r} \right\} \hat{\phi}.\end{aligned} \tag{7.100}$$

The angular momentum transport ($\hat{\phi}$) by the stress tensor can be explained by several mechanisms: magneto-rotational instability, gravitational instability, and asymmetric gravitational torque. However, the way of momentum loss in other components is not clear.

1.5 Jets

In accretion physics, the motivation was predominantly theoretical in nature. (*i.e.* , we knew material must fall into the potential wall of the compact object, conserving angular momentum ⇒ accretion), supported by a body of circumstantial evidence (spectra, luminosity, variability). We know why accretion happens.

In jet physics, the situation is reversed. We know that jets exist primarily from an observational point of view (unlike accretion flows, they are resolved), but we don't

know why.

$\Rightarrow$ Phenomenological approach to understanding jets

Phenomenology

a) jets in astrophysical systems

- classic radio loud AGN ($\geq$ 10%)
- X-ray binaries
  - black holes (essentially all)
  - neutron stars (Z-sources)
  - white dwarfs (some CVs)
- Gamma ray bursts (100%)
- Proto-stars
- Pulsars ?

The ultimate test for the presence of a jet is still the resolved image of an elongated (*i.e.* , collimated) structure pointing away from a point source.

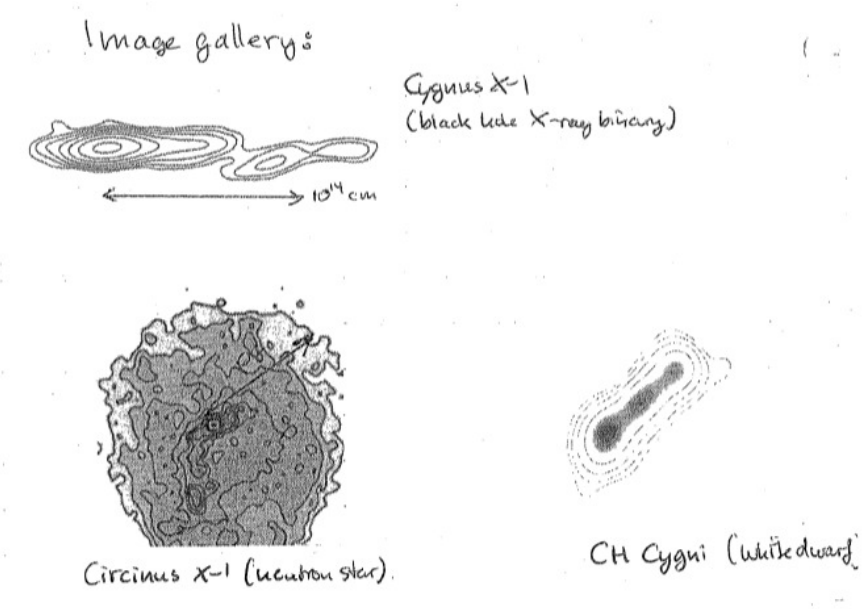

Figure 7.13 Top:Cygnus X-1, bottom-left: Circinus X-1 (neutron star), bottom-right: CH Cygni (White dwarf)

Morphology (See table (7.1))

b) Quantification:

Table 7.1 Fanaroff-Riley classification of radio galaxies (See fig.(7.14))

Type I	Type II
Brighter on smaller scales	Brighter on larger scales
Jet brighter than lobe	Jet dimmer than lobe
Often two-sided jets	Most often one-sided jets
Often bent jets	Straight jets

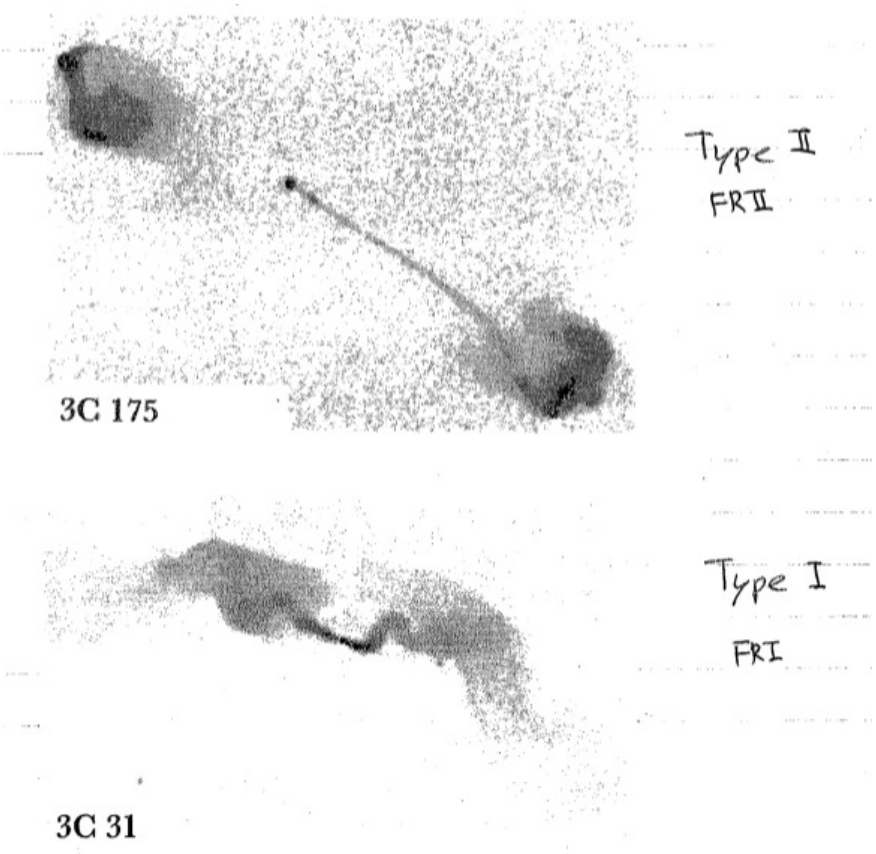

Figure 7.14 Top: FRII galaxy, bottom: FRI galaxy

Since AGN jets are the best studied species of relativistic jet, we will concentrate on them for a moment.

Spectra:

νL_ν spectrum indicates where the most energy comes out (See fig.(7.17)).

"Radio loud" AGN: Flat radio spectra from the nuclear region. $F_\nu \sim \nu^0$

Radio loudness,

$$R = \frac{L_{radio}}{L_{bol}} \simeq \frac{L_{5Ghz}}{L_B} \tag{7.101}$$

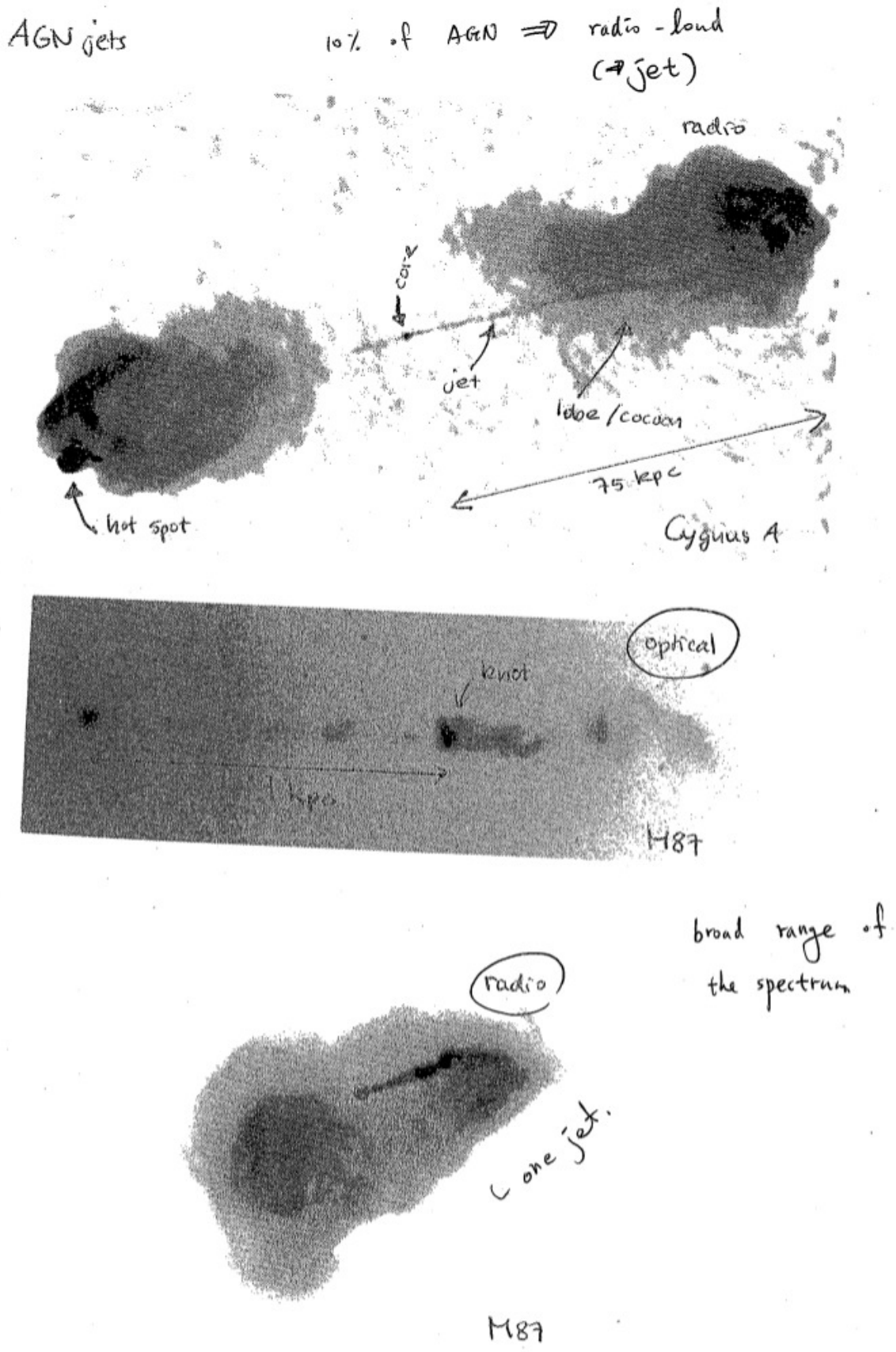

Figure 7.15 AGN jets

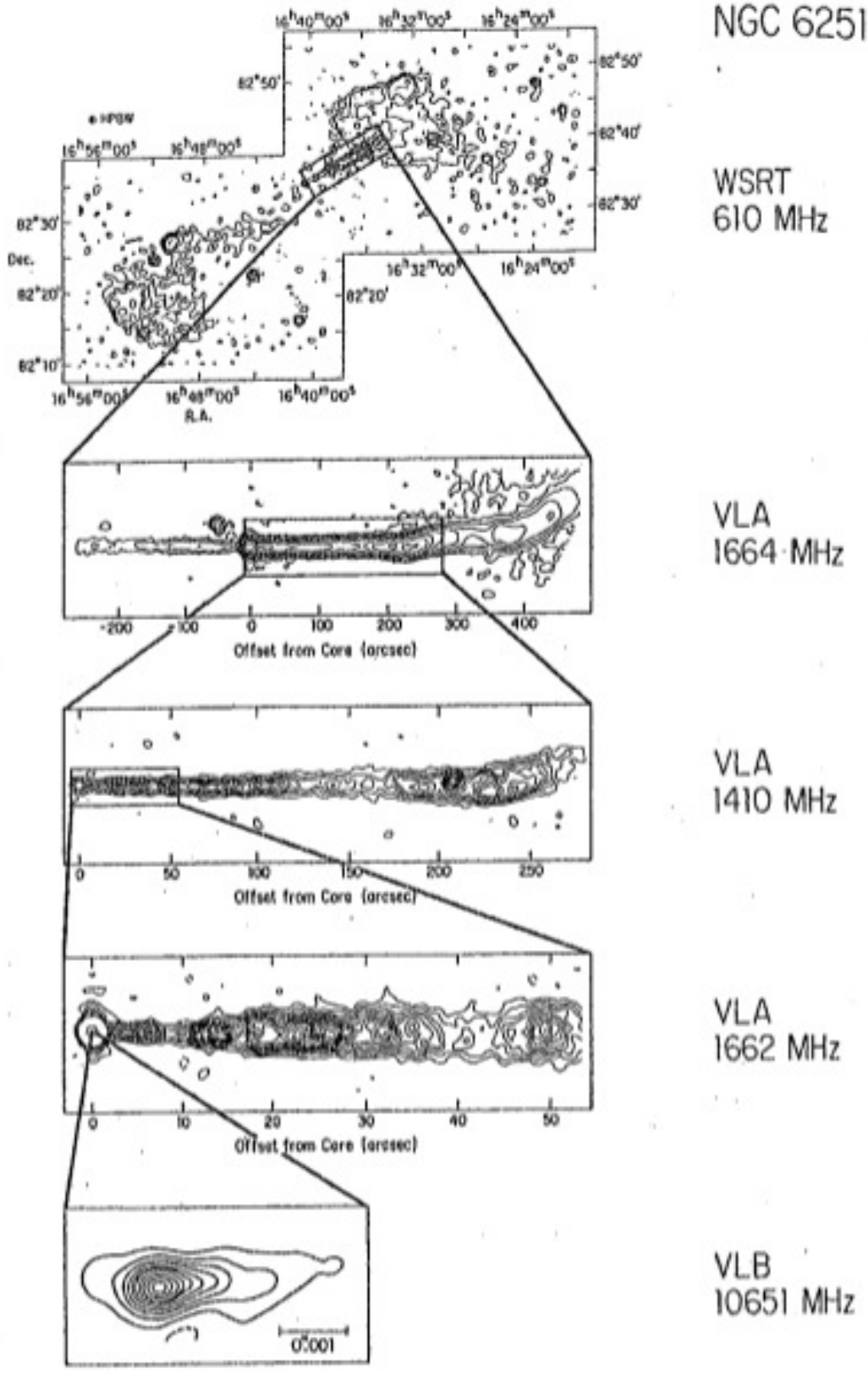

Figure 7.16 The FRI radio galaxy NGC 6251 at a succession of resolution and frequencies (courtesy A. Bridle). Although small displacements occur from scale to scale, overall the jet retains a remarkably constant alignment over a dynamic range in length scale of 10^6!

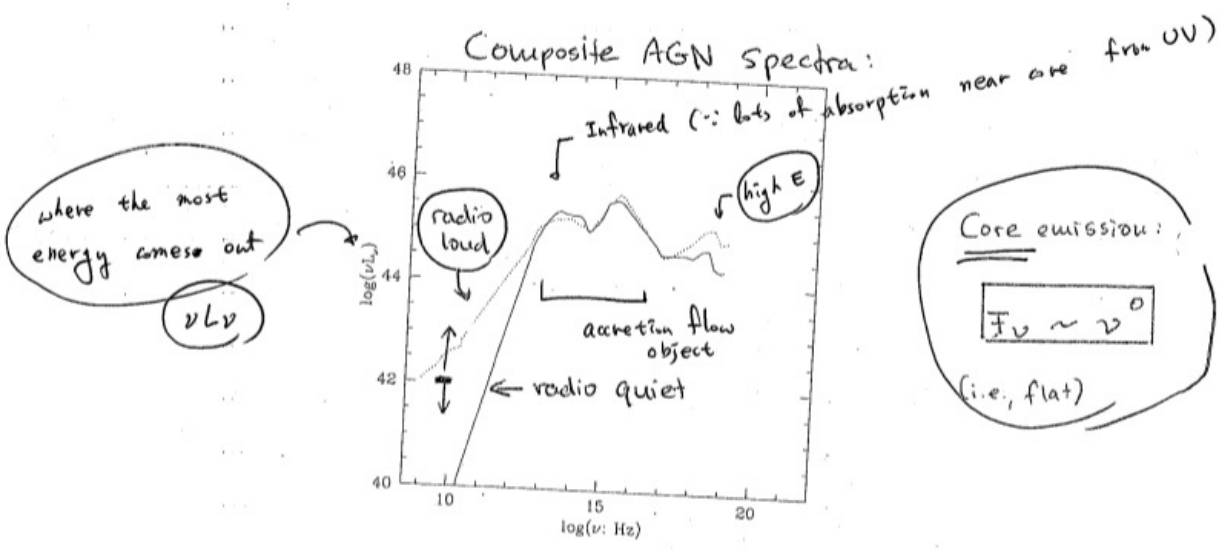

Figure 7.17 Composite AGN Spectra. Dotted line represents radio-loud AGN and solid line represents radio-quiet AGN.

where L_B is luminosity in B-band. We classify AGN as Radio loud, when $R > 2 \times 10^{-4}$.

$L_{radio} \sim$ few $\times 10^{30}$ to few $\times 10^{42}\,\mathrm{erg\,s^{-1}}$

BL-Lac objects and "blazars"

Some sources are completely dominated by jet emission, *i.e.* , the broad emission lines are hardly seen.

BL-Lacertae-objects and "blazars"

These objects, fig.(7.18), have pure power-law spectrum up to some cut-off frequency ν_{cut}. Furthermore, they have X-ray & γ-ray spectra of the same shape.

Extended emission:

- Jets show radio spectra with index $\alpha \approx 0.6$, where

$$F_\nu \propto \nu^{-\alpha} \tag{7.102}$$

  cf) core emission: $F_\nu \propto \nu^0$, *i.e.* flat spectrum

- Radio lobes show steeper spectra with $\alpha \approx 1 - 2$, since optically thin relatively to central region.

Polarization:

Jet emission is almost always polarized. The degree of polarization ranges from a few tenths of a percent to almost 70%.

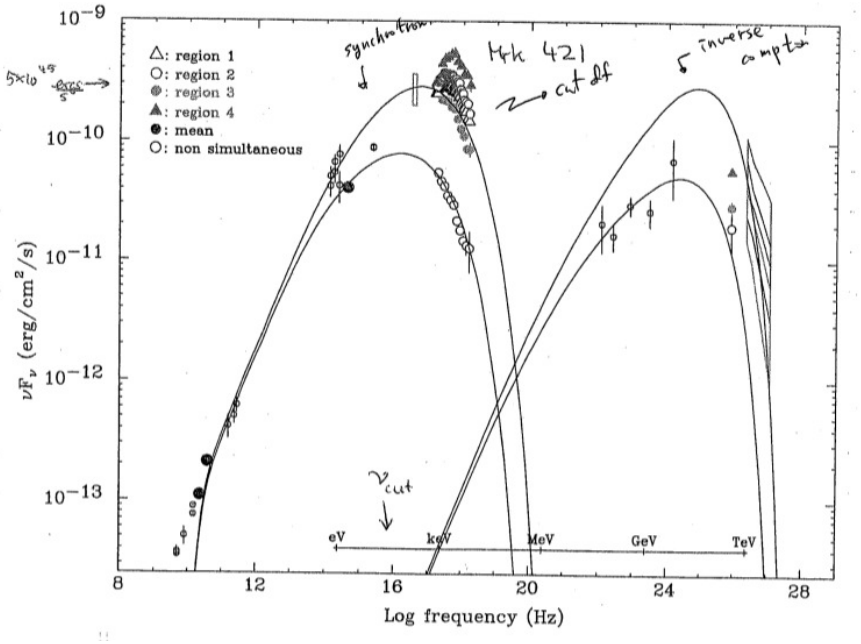

Figure 7.18 Spectrum of BL-Lac object

We observe strongly polarized power-law (non-thermal) emission across the entire electromagnetic spectrum.

Possible processes:

1) Synchrotron radiation

2) Inverse Compton emission

Answer: Both (Synchrotron at low and inverse compton at high frequencies)

This morphological dichotomy is a fundamental property of radio galaxies.

Evidence for relativistic motion

a) Proper motion (super-luminal motion)

(a) perceived distance traveled

$$\Delta x = v \cdot \sin\theta \cdot \Delta t \tag{7.103}$$

(b) perceived time elapsed

$$\Delta\tau = \frac{\Delta y}{c} = \frac{(c - v \cdot \cos\theta)\Delta t}{c} = (1 - \beta\cos\theta)\,\Delta t \tag{7.104}$$

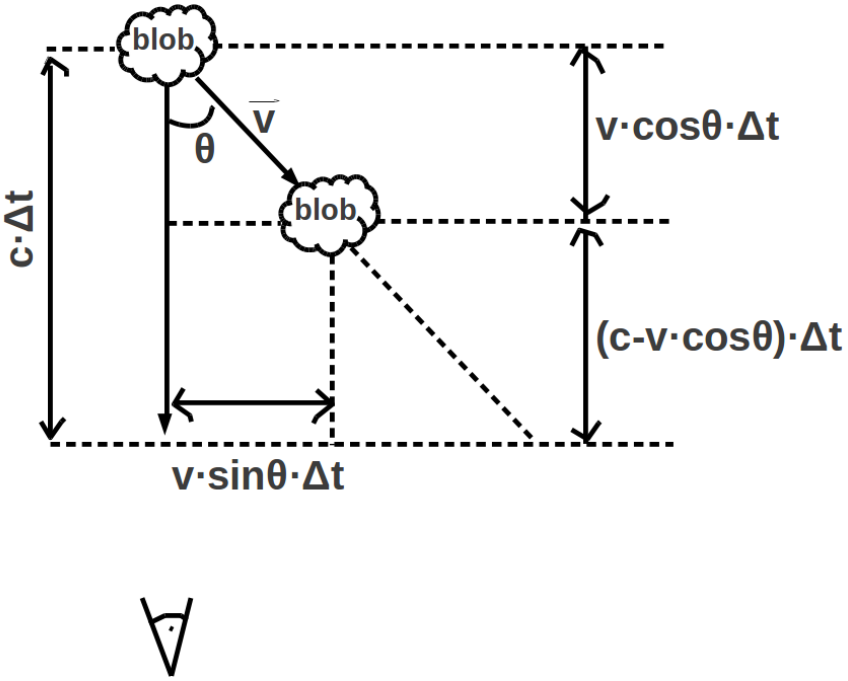

Figure 7.19 Super-luminal motion

$\Rightarrow$ perceived proper motion:

$$\therefore \quad \boxed{v_{obs} = \frac{\Delta x}{\Delta \tau} = \frac{v \cdot \sin\theta}{1 - \beta \cos\theta}} \tag{7.105}$$

or,

$$\boxed{\beta_{obs} = \frac{\beta \sin\theta}{1 - \beta \cos\theta}} \tag{7.106}$$

Recall $\beta < 1$,

$$\beta_{obs} = \frac{\beta \sin\theta}{1 - \beta(1 - \sin^2\theta)^{1/2}}$$

$$\Rightarrow \quad \frac{1}{\beta} = (1 - \sin^2)^{1/2} + \frac{\sin\theta}{\beta_{obs}} > 1 \tag{7.107}$$

$$\Rightarrow \quad \boxed{\sin\theta < \frac{2\beta_{obs}}{1 + \beta_{obs}} \quad \text{or} \quad \theta < \frac{2}{\beta_{obs}} \quad \text{for} \quad \beta_{obs} \gg 1} \tag{7.108}$$

Recall

$$\boxed{\beta\Gamma \geq \beta_{obs}} \tag{7.109}$$

where $\Gamma = \sqrt{1/(1-\beta^2)}$. Note that β_{obs} might not be a physical speed, *i.e.* , a pattern speed from a moving shock. Note that Superluminal motion is not a relativistic effect, it is purely a light-travel time effect. Most extreme blazars: $\beta_{obs} \sim 30 - 50$!

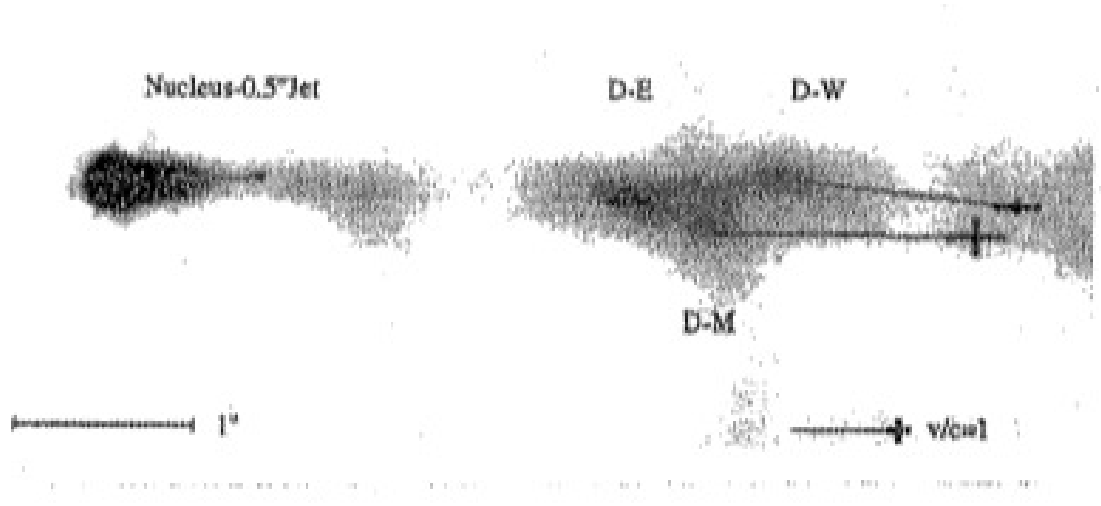

Figure 7.20 M87. $\beta_{obs} \sim 3 - 5$

b) **Relativistic Doppler boosting**: relativistic beaming + blue shift

FRII sources are almost always one-sided. This is easily understood as a consequence of Doppler boosting.

Assume each source has two equal jets traveling in opposite directions (jet and counter-jet). Each emits radiation at a rate L_ν in its own, co-moving frame. Doppler boosting implies that the detected luminosity is

$$L_{obs} = \delta^{k+\alpha} L_\nu \tag{7.110}$$

where k is what kind of object you're looking at, and δ is the Doppler factor,

$$\delta = \frac{1}{\Gamma(1 - \beta\cos\theta)} \tag{7.111}$$

In case of moving away, $\delta = \frac{1}{\Gamma(1+\beta\cos\theta)}$. Note that

$$\Rightarrow \begin{cases} \theta \ll 1 & \rightarrow \quad \delta \gg 1 \quad \text{for } \theta < 1/\Gamma \\ \theta \gg 1 & \rightarrow \quad \delta \sim 1/\Gamma \ll 1 \end{cases} \tag{7.112}$$

α is the spectral index ($F_\nu \propto \nu^{-\alpha}$), and

$$\begin{array}{ll} k = 2 & \text{(continuous emission)} \\ k = 3 & \text{(blob-emission)} \end{array}$$

and $\beta = v/c$, $\Gamma = 1/\sqrt{1-\beta^2}$, θ=angle to line-of-sight. The jet-to-counter-jet brightness ratio is then,

$$\frac{L_{obs,jet}}{L_{obs,counter-jet}} = \left(\frac{1+\beta\cos\theta}{1-\beta\cos\theta}\right)^{k+\alpha} \equiv l^{k+\alpha} \tag{7.113}$$

Note:

1) Γ cancels out (convenient)

2) L cancels out (distance independence !)

3) β and θ only enter as product $\Rightarrow$ can only measure $\beta \cdot \cos\theta$

$$\boxed{\beta \cdot \cos\theta = \frac{l-1}{l+1}} \tag{7.114}$$

Since we know $\beta < 1$ and $\cos\theta \leq 1$:

$$\beta \geq \frac{l-1}{l+1} \quad \text{and} \quad \cos\theta > \frac{l-1}{l+1} \tag{7.115}$$

Example: M87

$L_{obs,jet} \geq 380 \cdot L_{obs,counter-jet}$
$\Rightarrow \quad l_{obs} \geq 11$
$\Rightarrow \quad \beta \geq 0.83 \quad \text{and} \quad \theta < 34^\circ$
where $\Gamma \geq 2$

c) Variability

Some radio loud AGN (*e.g.* , blazars) vary on time scales of days and shorter across the entire spectrum.

Causality implies a source size limit of

$$\Delta r \leq c \cdot \Delta t \sim 10^{16}\,\mathrm{cm} \tag{7.116}$$

Note: the observed time Δt_{obs} is shorter by a factor δ^{-1} than the co-moving time,

$$\Delta t_{obs} = \Delta t_{co}/\delta \tag{7.117}$$

The emission is polarized and follows a roughly flat power-law $\Rightarrow$ optically thick synchrotron emission. For a typical luminosity of $10^{42}\,\mathrm{erg\,s^{-1}}$ at 5 Ghz, the surface brightness of the emission (observed) is

$$S_{\nu,obs} = \frac{L_{\nu,obs}}{(4\pi)(\pi\Delta r^2)} = 0.05\,\mathrm{erg\,cm^{-2}\,s^{-1}Hz^{-1}Sr^{-1}} \tag{7.118}$$

which corresponds to a brightness temperature of

$$T_{b,obs} = \frac{c^2}{2\nu^2 k} \cdot S_\nu \approx 10^{16} K \quad \text{(not reasonable)} \tag{7.119}$$

Recall from synchrotron theory of self-absorbed sources:

$$S_\nu = \frac{j_\nu}{\alpha_\nu} \propto B^{-1/2}\nu^{5/2} \tag{7.120}$$

where j_ν is emissivity and α_ν is absorption coefficient. Up to some maximum frequency ν_{peak}, so the bolometric radiation energy density is

$$u_{rad} \sim \frac{S_{peak}}{c} \propto B^{-1/2}\nu_{peak}^{5/2} \tag{7.121}$$

while the magnetic energy density follows

$$u_B = \frac{B^2}{8\pi} \propto B^2 \tag{7.122}$$

Now, recall from synchrotron and inverse Compton theory that losses are proportional to u_B and u_{rad}, respectively. If u_{rad} is ever larger than u_B, Compton losses grow exponentially (instability) and cool the particle distribution to the point where $u_{rad} \leq u_B$ again (this is called the "Compton catastrophe")

$\Rightarrow$ In synchrotron emitting sources: $u_B \geq u_{rad}$

We can re-write this, using $u_{rad} \sim B^{-1/2}\nu_{peak}^{5/2}$:

$$\begin{aligned} u_{rad}/u_B &< \text{const} \\ \Rightarrow B^{-5/2}\,\nu_{peak}^{5/2} &< \text{const} \\ B^{-1/2}\,\nu_{peak}^{1/2} &< \text{const} \quad \equiv \quad \mathrm{T_{max}} \end{aligned} \tag{7.123}$$

Plugging the expression for S_{peak} in, this gives

$$S_{peak} \sim B^{-1/2}\nu_{peak}^{5/2} < T_{max}\nu_{peak}^2 \tag{7.124}$$

or

$$T_{B,peak} = \frac{S_{peak}c^2}{2\,k\,\nu_{peak}^2} < T_{max} \approx 10^{12}\,K \tag{7.125}$$

Thus, the brightness temperature of a synchrotron emitting source is limited to

$$T_B < 10^{12}\,K \tag{7.126}$$

The only way to bring the observed 10^{16} K in line with this limit is relativistic motion:

1) $\Delta r_{obs} \propto \Delta t_{obs} \propto \Delta t \cdot \frac{1}{\delta}$
2) $\nu_{obs} \propto \nu \cdot \delta$
3) $L_{\nu,obs} \propto L_\nu \cdot \delta^{k+\alpha}$

$\Rightarrow \quad T_{obs} \propto \delta^{k+\alpha} \sim \delta^3$

$\Rightarrow \quad \delta \sim 10^{4/3} \sim 20$

d) Physical parameters

Given a physical size and luminosity, we can use synchrotron theory to constrain the physical conditions in the source.

Recall:

$$j_\nu \approx 10^{-18}\,p\,B^{(p+1)/2}\,\nu_{5GHz}^{-(p-1)/2}\,erg\,cm^{-3}\,s^{-1}Hz^{-1} \tag{7.127}$$

where p is pressure density in relativistic particles (erg cm^{-3}).

Example: M87, "knot A"

$L_{5Ghz} \approx 5 \times 10^{29}\,\mathrm{erg\,s^{-1}Hz^{-1}} \cdot \delta^{-2-\alpha}$

size: $\Delta r \approx 100\text{pc}$

$\rightarrow \quad j_{5Ghz} \approx 4 \times 10^{-33}\,\text{erg}\,\text{cm}^{-3}\,\text{s}^{-1}\text{Hz}^{-1} \quad \delta^{-2-\alpha}$

$\rightarrow \quad p\,B^{1.5} \approx 4 \times 10^{-15}\delta^{-2-\alpha}$

Without a way to measure B directly, we usually proceed to make the (usually poorly justified) assumption of equipartition:

$$\begin{aligned} p &\approx \frac{B^2}{8\pi} \\ \rightarrow p &\approx 2 \times 10^{-10}\,erg\,cm^{-3}\delta^{-10/7} \\ B &\approx 100\,\mu G\;\delta^{-5/7} \end{aligned} \tag{7.128}$$

We also know that $\Gamma \sim 5$ So roughly,

$$\boxed{L_{kin} \sim \left(4p + B^2/4\pi\right)\pi\Delta r^2\Gamma^2\beta^2 c} \tag{7.129}$$

$$\boxed{\sim 3 \times 10^{43}\,erg\,s^{-1}} \tag{7.130}$$

(Note: this is just an illustrative example, the numbers are order-of-magnitude accurate only.)

M87 is an FRI source, which is consistent with this kind of power estimate.

Recall from accretion section: $\dot{M}_{\text{Bondi}} \sim 0.03\,\text{M}_\odot\,\text{yr}^{-1}$

$$\boxed{L_{\text{Bondi}} \sim 2 \times 10^{43}\,\text{erg}\,\text{s}^{-1}} \tag{7.131}$$

compton scattering inverse compton scattering

1.6 Binary System

Kepler's Law

1. The orbit of every planet is an ellipse with the sun at one of two foci.

$$r = \frac{p}{1 + \epsilon\cos\theta}$$

where p=b^2/a (semi-latus rectum), $\epsilon = \sqrt{1 - (b/a)^2}$ (eccentricity).

2. A line joining a planet and the sun sweeps out equal area during equal intervals of time.

$$\frac{d}{dt}\left(\frac{1}{2}r^2\theta\right) = 0.$$

3. The square of the orbital period of a planet is directly proportional to the cube of the semi-major axis of its orbit.

$$T^2 = \frac{4\pi^2 a^3}{\mathrm{GM}}.$$

4. Center of Mass

$$r_1 M_1 = r_2 M_2 \tag{7.132}$$

Therefore,

$$r_1 = \frac{M_2}{M_1 + M_2}\, r \tag{7.133}$$

or,

$$r_2 = \frac{M_1}{M_1 + M_2}\, r \tag{7.134}$$

where $r = r_1 + r_2$. In this context, the Kepler's law can be expressed as,

$$\omega^2 = \frac{G\,(M_1 + M_2)}{a^3}, \tag{7.135}$$

where $\omega = 2\,\pi/T$.

5. Inclination angle: i If the normal vector of the orbital plane is inclined to the line of sight by an angle i, the Doppler velocity amplitudes we measure will be

$$|v_{1obs}| = |v_1| \sin i, \quad |v_{2obs}| = |v_2| \sin i. \tag{7.136}$$

Then,

$$\frac{M_2^3}{(M_1 + M_2)^2} \sin^3 i = \frac{\tau |v_{1obs}|^3}{2\pi\, G}, \tag{7.137}$$

where $\tau = 2\pi\, r_1/|v_1| = 2\pi\, r_2/|v_2|$. The detailed derivation is in Maoz (2009).

Tidal force

$$dF_{\text{Tidal}} = \frac{2GMmdr}{r^3}$$

Chapter 8

Cosmology

1 Hubble law

The relative velocity v between two galaxies that are separated by a large distance r is given by the Hubble law:

$$v = H_0 r, \tag{8.1}$$

where H_0 is the **Hubble constant**:

$$H_0 = (72 \pm 8)\,\mathrm{km\,s^{-1}\,Mpc^{-1}}. \tag{8.2}$$

Chapter 9

Particle Physics

Leptons: the lightest particles are spin-1/2 fermions that do not experience the strong nuclear force, but observe Pauli's exclusion principle.

	charged	neutrino
electronic	e^- $(0.511 Mev)^*$	ν_e
muonic	μ^- (105.6 MeV)	ν_μ
tauonic	τ^- (1777 MeV)	ν_τ

e^- are stable, the most common and least mass charged lepton in the universe.

Hadrons:

- Baryons: fermions that are strongly interacting.
  Greek means "heavy particles".
  The lightest and most familiar baryons are the proton and the neutron.
- Mesons: "messenger" particles made of an even number of quarks and antiquark.
  They are bosons.
  $\sigma^-, \omega^-, \rho -$ mesons, Pions(π) and kaons $(K^+, K^0, \bar{K}^0, K^-)$.

*the rest mass energy

Chapter 10

Mathematical physics

1 Mathematical physics

1.1 Moment of Inertia

Moment of inertia is the name given to rotational inertia, the rotational analog of mass for linear motion. It appears in the relationships for the dynamics of rotational motion. The moment of inertia must be specified with respect to a chosen axis of rotation. For a point mass, the moment of inertia is just the mass times the square of perpendicular distance to the rotation axis, $I = m\,r^2$. That point mass relationship becomes the basis for all other moment of inertia since any object can be built up from a collection of point masses. For the extended source, we have to integrate through the volume,

$$I = \int dI = \int_0^M r^2 dm \tag{10.1}$$

sphere

To derive the moment of inertia of a solid sphere of uniform density and radius R,

$$dI = r_\perp^2\, dm = r_\perp^2 \rho\, dV \tag{10.2}$$

where $r_\perp$ is the perpendicular distance to a point at $\vec{r}$ from the axis of rotation. Therefore, $r_\perp = |\vec{r}| \sin\theta$. Integrating over the volume,

$$\begin{aligned} I &= \int\int\int_V \rho\, r_\perp^2\, dV = \rho \int_0^{2\pi}\int_0^{\pi}\int_0^{R} (r\,\sin\theta)^2\, r^2\,\sin\theta dr d\theta d\phi \\ &= 2\pi\rho \int_0^{\pi} \sin^3\theta d\theta \int_0^{R} r^4 dr \qquad \leftarrow \text{substituting } u = \cos\theta \\ &= 2\pi\rho \frac{R^5}{5} \int_{-1}^{1} \left(1-u^2\right) du = \frac{4}{3}\pi R^3 \rho \left(\frac{2}{5}R^2\right) \\ &= \frac{2}{5} M R^2 \end{aligned} \tag{10.3}$$

where M is the total mass of the sphere.

1.2 Potential of Uniform Sphere

To be updated

$$U = -\frac{3}{5}\frac{G\,M}{R} \tag{10.4}$$

1.3 Fourier decomposition

Chapter 11

Instrument

1 Optical

- Angular resolution

$$\theta = 1.22 \frac{\lambda}{D}, \tag{11.1}$$

where a plane wave of wavelength λ passing through a circular aperture of diameter D.

2 Radio

3 X-ray

4 Infrared

Appendix A

Appendix

1 Astrophysical Constants

Table A.1.

Physical and Astrophysical constants

Constant	CGS unit	Constant	CGS unit
c_0 (speed of light in vacuum)	$2.99792458 \times 10^{10}$ cm s^{-1}	h (Plank constant)	$6.6260755 \times 10^{-27}$ erg s
e (electron charge)	$4.80320680 \times 10^{-10}$ esu	α (fine structure constant)	1/137.03598951
m_e (electron mass)	$9.1093897 \times 10^{-28}$ g	r_e (classical electron radius)	$2.81794092 \times 10^{-13}$ cm
m_p (proton mass)	1.672631×10^{-24} g	Bohr radius	$0.529177249 \times 10^{-8}$ cm
m_n (neutron mass)	$1.6749286 \times 10^{-24}$ g	G (gravitational const)	6.67259×10^{-8} $cm^3 g^{-1} s^{-2}$
m_d (deuteron mass)	$3.34358602 \times 10^{-24}$ g	G′(gravitational const) **	4.298 $M_\odot^{-1} pc^2 km^2 s^{-2} kpc^{-1}$
u (unified atomic mass)	$1.6605402 \times 10^{-24}$ g	N_A (Abogadro const)	6.0221367×10^{23} mol^{-1}
k (Boltzmann constant)	1.380658×10^{-16} erg K^{-1}	b (Wien disp. law const)	0.2897756 cm K
σ_{SB} (Stefan-Boltzman const)	5.67×10^{-5} erg $s^{-1} cm^{-2} K^{-4}$	AU (astronomical unit)	$1.4959787066 \times 10^{13}$ cm
Jy (Jansky)	10^{-23} erg s^{-1} cm^{-2} Hz^{-1}	pc (parsec)	$3.0856775807 \times 10^{18}$ cm
$M_\odot$ (Solar mass)	1.98892×10^{33} g	ly (light year)	0.9461×10^{18} cm
M_{Earth} (Earth mass)	5.97370×10^{27} g	ev (electron volt)	1.602×10^{-12} erg
M_{Moon} (Moon mass)	7.348×10^{25} g	Plank Mass	2.17671×10^{-5} g
$L_\odot$ (Solar luminosity)	3.846×10^{33} erg s^{-1}	Plank length	1.61605×10^{-33} cm
$R_\odot$ (Solar radius)	6.955×10^{10} cm	Plank time	5.39056×10^{-44} s
σ_T (Thompson Cross section)	$6.65246154 \times 10^{-25}$ cm^2	J (Joule)	10^7 erg
ϵ_0 (permittivity of vacuum) *	8.854×10^{-12} $C^2 m^{-2} N^{-1}$	N (Newton)	10^5 dyne
μ_0 (permeability of vacuum) *	$4\pi \times 10^{-7}$ H m^{-1}	yr (year)	3.155693×10^7 s
Tesla	10^4 Gauss		

* SI unit ; In cgs unit, ϵ_0 and μ_0 are unity.

** special unit

2 Vector Identity

$$
\begin{aligned}
\boldsymbol{a}\cdot(\boldsymbol{b}\times\boldsymbol{c}) &= \boldsymbol{b}\cdot(\boldsymbol{c}\times\boldsymbol{a}) = \boldsymbol{c}\cdot(\boldsymbol{a}\times\boldsymbol{b}) \\
\boldsymbol{a}\times(\boldsymbol{b}\times\boldsymbol{c}) &= (\boldsymbol{a}\cdot\boldsymbol{c})\,\boldsymbol{b} - (\boldsymbol{a}\cdot\boldsymbol{b})\,\boldsymbol{c} \\
(\boldsymbol{a}\times\boldsymbol{b})\cdot(\boldsymbol{c}\times\boldsymbol{d}) &= (\boldsymbol{a}\cdot\boldsymbol{c})\,(\boldsymbol{b}\cdot\boldsymbol{d}) - (\boldsymbol{a}\cdot\boldsymbol{d})\,(\boldsymbol{b}\cdot\boldsymbol{c}) \\
\nabla\times\nabla\psi &= 0 \\
\nabla\cdot(\nabla\times\boldsymbol{a}) &= 0 \\
\nabla\times(\nabla\times\boldsymbol{a}) &= \nabla\,(\nabla\cdot\boldsymbol{a}) - \nabla^2\boldsymbol{a} \\
\nabla\cdot(\psi\boldsymbol{a}) &= \boldsymbol{a}\cdot\nabla\psi + \psi\nabla\cdot\boldsymbol{a} \\
\nabla\times(\psi\boldsymbol{a}) &= \nabla\psi\times\boldsymbol{a} + \psi\nabla\times\boldsymbol{a} \\
\nabla\,(\boldsymbol{a}\cdot\boldsymbol{b}) &= (\boldsymbol{a}\cdot\nabla)\,\boldsymbol{b} + (\boldsymbol{b}\cdot\nabla)\,\boldsymbol{a} + \boldsymbol{a}\times(\nabla\times\boldsymbol{b}) + \boldsymbol{b}\times(\nabla\times\boldsymbol{a}) \\
\nabla\cdot(\boldsymbol{a}\times\boldsymbol{b}) &= \boldsymbol{b}\cdot(\nabla\times\boldsymbol{a}) - \boldsymbol{a}\cdot(\nabla\times\boldsymbol{b}) \\
\nabla\times(\boldsymbol{a}\times\boldsymbol{b}) &= \boldsymbol{a}\,(\nabla\cdot\boldsymbol{b}) - \boldsymbol{b}\,(\nabla\cdot\boldsymbol{a}) + (\boldsymbol{b}\cdot\nabla)\,\boldsymbol{a} - (\boldsymbol{a}\cdot\nabla)\,\boldsymbol{b}
\end{aligned}
$$

3 Vector Calculus

$$\int_V \nabla \cdot \boldsymbol{A}\, d^3x = \int_S \boldsymbol{A} \cdot \boldsymbol{n}\, da \qquad \text{(Divergence Theorem)}$$

$$\int_V \nabla \psi d^3x = \int_S \psi \boldsymbol{n}\, da$$

$$\int_V \nabla \times \boldsymbol{A}\, d^3x = \int_S \boldsymbol{n} \times \boldsymbol{A}\, da$$

$$\int_V \left(\phi \nabla^2 \psi + \nabla\phi \cdot \nabla\psi\right) d^3x = \int_S \phi \boldsymbol{n} \cdot \nabla\psi da \qquad \text{(Green's first identity)}$$

$$\int_V \left(\phi \nabla^2 \psi - \psi \nabla^2 \phi\right) d^3x = \int_S (\phi \nabla\psi - \psi\nabla\phi) \cdot \boldsymbol{n}\, da \qquad \text{(Green's theorem)}$$

$$\int_S (\nabla \times \boldsymbol{A}) \cdot \boldsymbol{n}\, da = \oint_C \boldsymbol{A} \cdot d\boldsymbol{l} \qquad \text{(Stokes's theorem)}$$

$$\int_S \boldsymbol{n} \times \nabla\psi da = \oint_C \psi d\boldsymbol{l}$$

4 Coordinate System

4.1 Cartesian (x,y,z)

$$
\begin{aligned}
\nabla\psi &= \frac{\partial\psi}{\partial x}\hat{\boldsymbol{x}} + \frac{\partial\psi}{\partial y}\hat{\boldsymbol{y}} + \frac{\partial\psi}{\partial z}\hat{\boldsymbol{z}} \\
\nabla\cdot\boldsymbol{A} &= \frac{\partial A_x}{\partial x} + \frac{\partial A_y}{\partial y} + \frac{\partial A_z}{\partial z} \\
\nabla\times\boldsymbol{A} &= \left(\frac{\partial A_z}{\partial y} - \frac{\partial A_y}{\partial z}\right)\hat{\boldsymbol{x}} + \left(\frac{\partial A_x}{\partial z} - \frac{\partial A_z}{\partial x}\right)\hat{\boldsymbol{y}} + \left(\frac{\partial A_y}{\partial x} - \frac{\partial A_x}{\partial y}\right)\hat{\boldsymbol{z}} \\
(\boldsymbol{A}\cdot\nabla)\,\boldsymbol{B} &= \left(A_x\frac{\partial B_x}{\partial x} + A_y\frac{\partial B_x}{\partial y} + A_z\frac{\partial B_x}{\partial z}\right)\hat{\boldsymbol{x}} + \left(A_x\frac{\partial B_y}{\partial x} + A_y\frac{\partial B_y}{\partial y} + A_z\frac{\partial B_y}{\partial z}\right)\hat{\boldsymbol{y}} \\
&\quad + \left(A_x\frac{\partial B_z}{\partial x} + A_y\frac{\partial B_z}{\partial y} + A_z\frac{\partial B_z}{\partial z}\right)\hat{\boldsymbol{z}} \\
\nabla^2\psi &= \frac{\partial^2\psi}{\partial x^2} + \frac{\partial^2\psi}{\partial y^2} + \frac{\partial^2\psi}{\partial z^2} \\
\nabla\cdot\boldsymbol{T}_{i,j} &= \left(\frac{\partial T_{xx}}{\partial x} + \frac{\partial T_{yx}}{\partial y} + \frac{\partial T_{zx}}{\partial z}\right)\hat{\boldsymbol{x}} + \left(\frac{\partial T_{xy}}{\partial x} + \frac{\partial T_{yy}}{\partial y} + \frac{\partial T_{zy}}{\partial z}\right)\hat{\boldsymbol{y}} \\
&\quad + \left(\frac{\partial T_{xz}}{\partial x} + \frac{\partial T_{yz}}{\partial y} + \frac{\partial T_{zz}}{\partial z}\right)\hat{\boldsymbol{z}}
\end{aligned}
$$

4.2 Cylindrical (ρ,ϕ,z)

$$
\begin{aligned}
\nabla\psi &= \frac{\partial\psi}{\partial\rho}\hat{\boldsymbol{\rho}} + \frac{1}{\rho}\frac{\partial\psi}{\partial\phi}\hat{\boldsymbol{\phi}} + \frac{\partial\psi}{\partial z}\hat{\boldsymbol{z}} \\
\nabla\cdot\boldsymbol{A} &= \frac{1}{\rho}\frac{\partial}{\partial\rho}\left(\rho A_\rho\right) + \frac{1}{\rho}\frac{\partial A_\phi}{\partial\phi} + \frac{\partial A_z}{\partial z} \\
\nabla\times\boldsymbol{A} &= \left(\frac{1}{\rho}\frac{\partial A_z}{\partial\phi} - \frac{\partial A_\phi}{\partial z}\right)\hat{\boldsymbol{\rho}} + \left(\frac{\partial A_\rho}{\partial z} - \frac{\partial A_z}{\partial\rho}\right)\hat{\boldsymbol{\phi}} + \frac{1}{\rho}\left(\frac{\partial}{\partial\rho}\left(\rho A_\phi\right) - \frac{\partial A_\rho}{\partial\phi}\right)\hat{\boldsymbol{z}} \\
(\boldsymbol{A}\cdot\nabla)\,\boldsymbol{B} &= \left(A_\rho\frac{\partial B_\rho}{\partial\rho} + \frac{A_\phi}{\rho}\frac{\partial B_\rho}{\partial\phi} + A_z\frac{\partial B_\rho}{\partial z} - \frac{A_\phi B_\phi}{\rho}\right)\hat{\boldsymbol{\rho}} \\
&\quad + \left(A_\rho\frac{\partial B_\phi}{\partial\rho} + \frac{A_\phi}{\rho}\frac{\partial B_\phi}{\partial\phi} + A_z\frac{\partial B_\phi}{\partial z} + \frac{A_\phi B_\rho}{\rho}\right)\hat{\boldsymbol{\phi}} \\
&\quad + \left(A_\rho\frac{\partial B_z}{\partial\rho} + \frac{A_\phi}{\rho}\frac{\partial B_z}{\partial\phi} + A_z\frac{\partial B_z}{\partial z}\right)\hat{\boldsymbol{z}} \\
\nabla^2\psi &= \frac{1}{\rho}\frac{\partial}{\partial\rho}\left(\rho\frac{\partial\psi}{\partial\rho}\right) + \frac{1}{\rho^2}\frac{\partial^2\psi}{\partial\phi^2} + \frac{\partial^2\psi}{\partial z^2} \\
\nabla\cdot\boldsymbol{T}_{i,j} &= \left\{\frac{1}{\rho}\frac{\partial}{\partial\rho}(\rho\, T_{\rho z}) + \frac{1}{\rho}\frac{\partial T_{\phi z}}{\partial\phi} + \frac{\partial T_{zz}}{\partial z}\right\}\hat{\boldsymbol{\rho}} \\
&\quad + \left\{\frac{1}{\rho}\frac{\partial}{\partial\rho}(\rho\, T_{\rho\rho}) + \frac{1}{\rho}\frac{\partial T_{\phi\rho}}{\partial\phi} + \frac{\partial T_{z\rho}}{\partial z} - \frac{T_{\phi\phi}}{\rho}\right\}\hat{\boldsymbol{\phi}} \\
&\quad + \left\{\frac{\partial T_{\rho\phi}}{\partial\rho} + \frac{1}{\rho}\frac{\partial T_{\phi\phi}}{\partial\phi} + \frac{\partial T_{z\phi}}{\partial z} + \frac{T_{\phi\rho} + T_{\rho\phi}}{\rho}\right\}\hat{\boldsymbol{z}}
\end{aligned}
$$

4.3 Spherical (r,θ,ϕ)

$$
\begin{aligned}
\nabla\psi &= \frac{\partial\psi}{\partial r}\hat{\boldsymbol{r}} + \frac{1}{r}\frac{\partial\psi}{\partial\theta}\hat{\boldsymbol{\theta}} + \frac{1}{r\sin\theta}\frac{\partial\psi}{\partial\phi}\hat{\boldsymbol{\phi}} \\
\nabla\cdot\boldsymbol{A} &= \frac{1}{r^2}\frac{\partial}{\partial r}\left(r^2 A_r\right) + \frac{1}{r\sin\theta}\frac{\partial}{\partial\theta}\left(\sin\theta A_\theta\right) + \frac{1}{r\sin\theta}\frac{\partial A_\phi}{\partial\phi} \\
\nabla\times\boldsymbol{A} &= \frac{1}{r\sin\theta}\left(\frac{\partial}{\partial\theta}\left(\sin\theta A_\phi\right) - \frac{\partial A_\theta}{\partial\phi}\right)\hat{\boldsymbol{r}} + \left(\frac{1}{r\sin\theta}\frac{\partial A_r}{\partial\phi} - \frac{1}{r}\frac{\partial}{\partial r}\left(rA_\phi\right)\right)\hat{\boldsymbol{\theta}} \\
&\quad + \frac{1}{r}\left(\frac{\partial}{\partial r}\left(rA_\theta\right) - \frac{\partial A_r}{\partial\theta}\right)\hat{\boldsymbol{\phi}} \\
(\boldsymbol{A}\cdot\nabla)\,\boldsymbol{B} &= \left(A_r\frac{\partial B_r}{\partial r} + \frac{A_\theta}{r}\frac{\partial B_r}{\partial\theta} + \frac{A_\phi}{r\,\sin\theta}\frac{\partial B_r}{\partial\phi} - \frac{A_\theta B_\theta + A_\phi B_\phi}{r}\right)\hat{\boldsymbol{r}} \\
&\quad + \left(A_r\frac{\partial B_\theta}{\partial r} + \frac{A_\theta}{r}\frac{\partial B_\theta}{\partial\theta} + \frac{A_\phi}{r\,\sin\theta}\frac{\partial B_\theta}{\partial\phi} + \frac{A_\theta B_r - A_\phi B_\phi\,\cot\theta}{r}\right)\hat{\boldsymbol{\theta}} \\
&\quad + \left(A_r\frac{\partial B_\phi}{\partial r} + \frac{A_\theta}{r}\frac{\partial B_\phi}{\partial\theta} + \frac{A_\phi}{r\,\sin\theta}\frac{\partial B_\phi}{\partial\phi} + \frac{A_\phi B_r + A_\phi B_\theta\,\cot\theta}{r}\right)\hat{\boldsymbol{\phi}} \\
\nabla^2\psi &= \frac{1}{r^2}\frac{\partial}{\partial r}\left(r^2\frac{\partial\psi}{\partial r}\right) + \frac{1}{r^2\sin\theta}\frac{\partial}{\partial\theta}\left(\sin\theta\frac{\partial\psi}{\partial\theta}\right) + \frac{1}{r^2\sin^2\theta}\frac{\partial^2\psi}{\partial\phi^2} \\
&\quad \text{Note that } \frac{1}{r^2}\frac{\partial}{\partial r}\left(r^2\frac{\partial\psi}{\partial r}\right) \equiv \frac{1}{r}\frac{\partial^2}{\partial r^2}\left(r\psi\right) \\
\nabla\cdot\boldsymbol{T}_{i,j} &= \left\{\frac{\partial T_{rr}}{\partial r} + \frac{1}{r}\frac{\partial T_{r\theta}}{\partial\theta} + \frac{1}{r\sin\theta}\frac{\partial T_{r\phi}}{\partial\phi} + \frac{2\,T_{rr} + \cot\theta\,T_{r\theta} - T_{\theta\theta} - T_{\phi\phi}}{r}\right\}\hat{\boldsymbol{r}} \\
&\quad + \left\{\frac{\partial T_{\theta r}}{\partial r} + \frac{1}{r}\frac{\partial T_{\theta\theta}}{\partial\theta} + \frac{1}{r\sin\theta}\frac{\partial T_{\theta\phi}}{\partial\phi} + \frac{T_{r\theta} + 2T_{\theta r} + \cot\theta(T_{\theta\theta} - T_{\phi\phi})}{r}\right\}\hat{\boldsymbol{\theta}} \\
&\quad + \left\{\frac{\partial T_{\phi r}}{\partial r} + \frac{1}{r}\frac{\partial T_{\phi\theta}}{\partial\theta} + \frac{1}{r\sin\theta}\frac{\partial T_{\phi\phi}}{\partial\phi} + \frac{T_{r\phi} + 2T_{\phi r} + \cot\theta(T_{\theta\phi} + T_{\phi\theta})}{r}\right\}\hat{\boldsymbol{\phi}}.
\end{aligned}
$$

5 Theoretical & Observational Tools

to be described

5.1 Codes

to be described

Particle

Grid

Hybrid

FLASH, ZEUS, ATHENA, GASOLIN, GADGET, GIZMO, CMHOG, AREPO

Bibliography

binney, j., & tremaine, s. 1987, galactic dynamics

Castor, J., McCray, R., & Weaver, R. 1975, ApJ, 200, L107

Dalgarno, A., & McCray, R. A. 1972, ARA&A, 10, 375

Kim, D.-W., & Pellegrini, S., eds. 2012, Astrophysics and Space Science Library, Vol. 378, Hot Interstellar Matter in Elliptical Galaxies

Maoz, S. 2009, Astrophysics in a Nutshell

Okuda, T., Fujita, M., & Sakashita, S. 1997, PASJ, 49, 679

Schure, K. M., Kosenko, D., Kaastra, J. S., Keppens, R., & Vink, J. 2009, A&A, 508, 751

shakura, n. i., & sunyaev, r. a. 1973, A&A, 24, 337

Stone, J. M., Pringle, J. E., & Begelman, M. C. 1999, MNRAS, 310, 1002